# Simultaneous pH and EC control in hydroponics through real-time manipulation of the ammonium-to-nitrate ratio in the nutrient solution

Roger Bosman
17306290

Department of Chemical Engineering
University of Pretoria

CVD 800

2024-03-15

# Abstract

A control scheme was developed whereby the pH and EC of the system was controlled by the simultaneous dosing of nutrient solutions of ammonium and nitrate in different ratios. By following this approach, the proposed system eliminates the need for a dedicated pH dosing reservoir and allows the system to reap the benefits of ammonium/nitrate nutrition.

The first step in developing the control algorithm was to understand the physiology of plants relevant to the uptake of nutrients (specifically nitrogen). This revealed that in order to transit from the soil solution to the xylem vessel, nutrients must pass through semipermeable cell membranes in the roots. Two mechanisms were identified for achieving this: carrier transport and channel transport. These two mechanisms provide the basis for the selective uptake of nutrients. Although carrier transport is the more selective of the two, ion channels represent the bulk of transport. Channel transport is driven by proton pumps which pump $H^+$ cations out of the cytosol into the apoplast, creating the pH fluctuations characteristic of nutrient absorption. It was made apparent that nutrient uptake was therefore a function of the genetic predisposition of the plant, the concentration of nutrients in the solution, the growth stage of the plant, and the ratio of nutrients in the solution. Once the mechanism by which nutrients are absorbed was understood, a review of hydroponic literature was conducted in order to identify the best practices when conducting experiments. This suggested that for kale, pH should be maintained between 5 and 7 (preferably 6) and that EC must be kept in the range 2 to 3 mS/cm. Finally, other studies dealing with the nitrogen uptake of leafy vegetables (with an emphasis on *Brassica*) were reviewed. It was found that, while seedlings typically enjoyed high ammonium concentrations, mature plants displayed signs of ammonium toxicity (like inhibited growth) at ammonium-to-nitrate ratios beyond 50 % but showed improved growth/nutritional qualities in the range 0 % to 50 %. Moreover, kinetic models were found that detail the uptake rates of ammonium and nitrate as their respective concentrations change.

These kinetic models were validated by performing a series of confirmatory experiments. These consisted of batch experiments conducted in an aeroponic hydroponic system. Having confirmed the validity of the literature relations, the kinetic models, in conjunction with other physiological parameters, were then used to develop a computer model of a kale plant. This model was used to tune the controller settings for the control systems.

Once a suitable controller had been developed based on the dynamic simulation, the controller parameters were applied to a hydroponic ebb-and-flow system to assess the efficacy of the proposed control scheme. Three experimental runs were conducted with

the purpose of testing the proposed control system on *Brassica oleracea* var. *acephala*. These are collectively referred to as the control system experiments. The first was an ideal case under sterile conditions, the second was under non-sterile conditions where bacteria were allowed to colonise the plant roots, and the last was a baseline run where nitrate was applied as the only nitrogen source. The system was able to control pH to within 0.5 of the set point (in this case 6.1) while EC control was sufficient to ensure that a steady stream of nutrients were available to the plants at all times. Relative growth rates were fast at maximum average values of between 0.20 $day^{-1}$ and 0.21 $day^{-1}$ for all of the runs and the yield of organic leaf matter was essentially the same across all the runs at 83 % to 86 % of total plant mass. Finally, the plants grown under the proposed control system were observed to exhibit some improvement in protein and chlorophyll content while the other nutritional characteristics considered were essentially unchanged between treatments. This was all accomplished without having to add any additional toxic ions like $Cl^-$ and $Na^+$ as is the case in conventionally controlled systems.

# Contents

# List of Figures

# List of Tables

# 1 Introduction

For much of the last century, nitrogen nutrition in hydroponics has been dominated by nitrates (Bugbee, 2004; Hoagland & Arnon, 1938; Ramazzotti *et al*, 2013). However, research has highlighted that many potential benefits can be had by adding ammonium into the mix with nitrate (Fallovo *et al*, 2006; Song, G Li, *et al*, 2016; Song, L Li, *et al*, 2017; Wang *et al*, 2022). These include potentially increased growth rates, greater concentrations of some minerals and phytochemicals, increased protein concentrations, and the reduction in carcinogenic nitrate within the edible organs of the plant (Song, L Li, *et al*, 2017; Tabatabaei, Yusefi & Hajiloo, 2008; Zhu *et al*, 2018). Despite these benefits, the spectre of ammonium toxicity – the wilting and yellowing of leaves, reduction of growth rate, and sometimes even the death of the plant, when ammonium concentrations grow too large or the ratio of ammonium-to-nitrate grows too high (Assimakopoulou *et al*, 2019; Fallovo *et al*, 2006; Wang *et al*, 2022; Zhang *et al*, 2007) – has served to constrain the use of ammonium more liberally in hydroponics (Bugbee, 2004). Although most common nutrient formulations add ammonium to the mix with the intention of moderating the pH change of the system, the amounts are paltry when compared to the amount of nitrate supplied and ultimately necessitate direct pH control anyway (Hoagland & Arnon, 1938; Ramazzotti *et al*, 2013).

As stated earlier, ammonium is often added to temper the pH response, though this is seldom relied on as a dedicated pH control strategy. An example of a more sophisticated use of ammonium to control pH is the study by Scherholz & Curtis (2013) in which an attempt was made to control pH through the addition of ammonium and nitrate to an algae culture in the hope that the simultaneous consumption of both would maintain a constant pH. Although failing when conducted as a batch experiment, the system was able to control pH when a fed batch system was implemented whereby ammonium nitrate was dosed to a nitrate medium containing the algae. Algae have the tendency to consume solely ammonium if given the opportunity (Fernández & Cárdenas, 1982; Florencio & Vega, 1983). As such, adding ammonium in the presence of nitrate has an immediate pH effect as the algae switch to ammonium nutrition before going back to consuming nitrate after the ammonium is depleted. Unlike algae, terrestrial plants tend to consume ammonium and nitrate in ratios corresponding to their concentration in the root zone (Song, G Li, *et al*, 2016), making pH control through nutrient manipulation somewhat more nuanced. Moreover, if too much ammonium is present, this can have potentially lethal implications for the plants in the system as they will start suffering from ammonium toxicity (Assimakopoulou *et al*, 2019; Britto & Kronzucker, 2002; Cramer & Lewis, 1993; Wang *et al*, 2022). This point alone discourages people from using ammonium in hydroponics, foregoing the possible benefits of operating the system at an appropriate

ammonium-to-nitrate ratio.

The aim of this research was to develop a system whereby ammonium and nitrate are supplied in such a ratio that the benefits of ammonium nutrition are achieved without inducing symptoms of ammonium toxicity in *Brassica oleracea* var. *acephala*. The choice of *B. oleraceae* var. *acephala* as the subject organism was based on the previous expertise regarding the plant in the research group (van Rooyen & Nicol, 2021; van Rooyen & Nicol, 2022a; van Rooyen & Nicol, 2022b), its tolerance of a wide range of electrical conductivities (Patel, 2022; Velazquez-Gonzalez *et al*, 2022), and its recent popularity as a superfood (Dunja Šamec & Salopek-Sondi, 2019). It was postulated that this could be achieved by supplying ammonium and nitrate in a ratio that maintains the pH while avoiding ammonium toxicity. This aim was supported by three objectives. Firstly, the preference of kale for ammonium and nitrate had to be quantified. Secondly, the pH effect of the absorption and assimilation of each of the two nitrogenous species had to be quantified. Understanding these two relationships allowed for the calculation of the pH homeostasis point – the ammonium to nitrate ratio where the pH rise due to the absorption of nitrate is cancelled out by the pH drop from the absorption of ammonium. Finally, having proven that the pH homeostasis point is not in the ammonium concentration range where ammonium toxicity begins to manifest, a control algorithm was developed to maintain this ratio without the need to explicitly measure the concentration of either ion.

In order to fulfil these objectives, a detailed literature study was first carried out to ascertain the exact mechanism by which plants absorb nutrients from the solution surrounding their roots. Having identified the various mechanisms used by plants to absorb different ions, and in doing so confirmed that plants are selective of the ions they uptake, the uptake kinetics for kale were found from literature. These kinetics, in conjunction with knowledge regarding the pH effect on the root zone of the absorption and assimilation of nitrate and ammonium, were used to develop a dynamic computer model of the plant. This model was then used to develop a control algorithm for the system. Finally, this control system was trialled on an ebb-and-flow hydroponic system to confirm its efficacy under both ideal conditions and in the face of bacterial infection. The results of the control system were then compared to a run fed purely on nitrate in order to ensure that the use of ammonium did not compromise growth or yield, and to see what benefits were gained by the application of ammonium.

# 2 Theory

## 2.1 Plant physiology

Underpinning this whole study are the nitrogen uptake characteristics of kale. However, in order to understand the nitrogen uptake characteristics of kale, one must first understand the mechanisms by which plants absorb nutrients and transport them through their tissues. This shall be broken down into a discussion of the plant physiology relevant to the movement of nutrients within a plant, followed by a more detailed discussion regarding the exact mechanisms responsible for the absorption of nutrients from the soil into the roots. Emphasis will be given to the transport of $NH_4^+$ and $NO_3^-$ as these two inorganic forms of nitrogen represent the most common source of nitrogen for plants (AJ Miller & Cramer, 2004; Masclaux-Daubresse *et al*, 2010).

### 2.1.1 The plant cell

Before delving into the structure of plants and the mechanisms by which they absorb nutrients, it is necessary to first consider the basic structure of a plant cell. A diagram of a plant cell is shown in Figure 1.

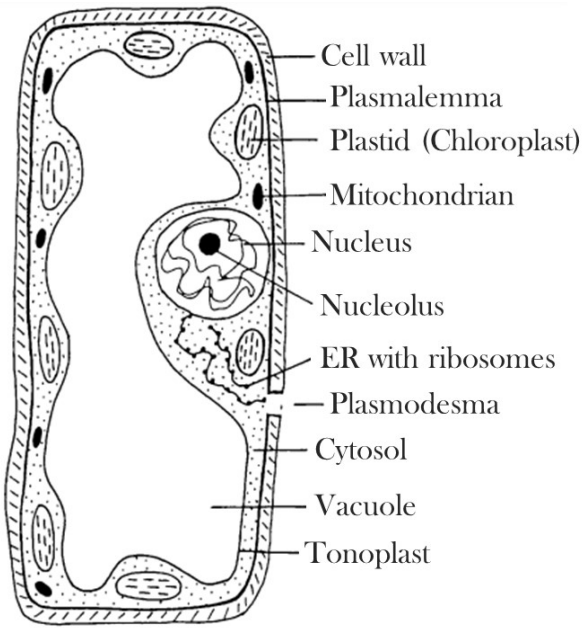


**Figure 1:** Depiction of a plant cell. This will be more-or-less the same for all living cells in a plant with the exception that plastids will not be present in root cells (adapted from Mengel, Kirkby, *et al* (2001: 113)).

Starting from the inside out, the largest organelle within the plant cell is the vacuole. This is a large reservoir of water in the middle of the cell that helps maintain cell turgor as well as store inorganic nutrients (particularly nitrates) and smaller amounts of other metabolic products and organic building blocks (Mengel, Kirkby, *et al*, 2001: 113). Other organelles include the nucleus where genetic information is stored, the mitochondrion which plays a part in energy generation, ribosomes which build proteins, and plastids (chloroplasts) which contain chlorophyll and convert $CO_2$ and water to glucose in the presence of sunlight.

These organelles are suspended in the cytoplasm, which is separated from the vacuole by a semipermeable membrane called the tonoplast. The cytoplasm without any organelles is called the cytosol. Every organelle in the cytoplasm is separated from the cytosol by semipermeable membranes (Mengel, Kirkby, *et al*, 2001: 113). The cytoplasm itself is then surrounded by a semipermeable membrane known as the plasmalemma (also known as the cell membrane), which controls the movement of materials into and out of the cell. The plasmalemma is made up primarily of phospholipids. These form a bilayer which is polar in the middle and unpolar on the outside. As such, the phospholipid sections are hydrophobic and do not allow polar molecules like water to pass through. The membrane is interspersed with proteins, most of which function as transport proteins, channel proteins, or redox proteins (Mengel, Kirkby, *et al*, 2001: 116). An illustration to this is given in Figure 2.

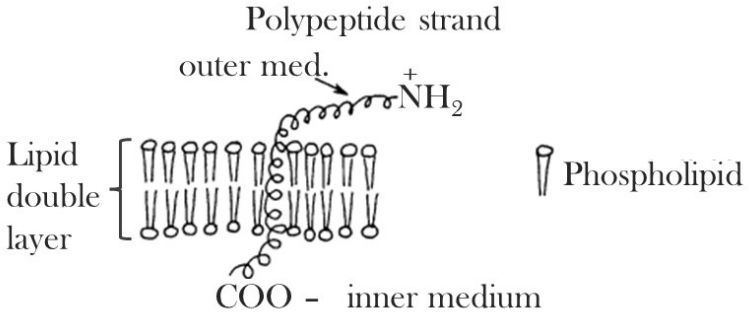


**Figure 2:** Phospholipid double-layer and an embedded protein chain (adapted from Mengel, Kirkby, *et al* (2001: 116)).

The structure of the plasmalemma and its proteins will become relevant in the following sections. Finally, the whole cell is surrounded by a cell wall.

The cell wall is primarily comprised of cellulose and hemicellulose (Mengel, Kirkby, *et al*, 2001: 112). The cellulose tends to aggregate into bundles known as microfibrils. Between these microfibrils are pores of diameter 4 to 8 nm. Because of these pores, cell walls are permeable to the movement of water and solutes, barring anything too large to fit

through the pores, such as bacteria (Hopmans & Bristow, 2002: 121). Figure 3 shows the porous structure of the cell wall.

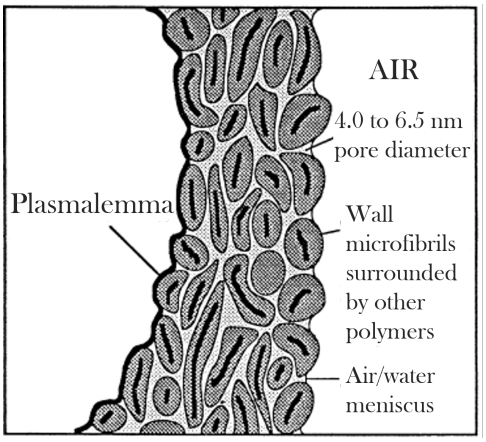


**Figure 3:** Cross section of a cell at the cytoplasm-cell wall boundary (adapted from Hopmans & Bristow (2002: 121)).

Looking at Figure 3 and its accompanying description, it is easy to assume that plant cells are completely self-enclosed units that are stacked together like bricks to make plant matter. However, this is not the case. In order to accurately describe the plant cell and how it fits into nutrient transport it is necessary to briefly look at how plant cells interact with one another. There are two aspects to this.

Firstly, although each cell has its own cell wall, the cell walls of neighbouring cells are bound together by the middle lamella, which is like cement holding the cells together (The Editors of Encyclopaedia Britannica, 2022). As such, the cell wall is more like a fibrous lattice into which the cells themselves slot. A visual analogy would be to look at a brick wall. The cells are the bricks while the cell wall is the mortar around the bricks. As such, the cell walls form a continuous system of porous material through which oxygen, $CO_2$, water, nutrients, and other materials diffuse freely. The whole cell wall region in a plant's tissue is known as the apoplast, literally meaning "free space" (Mengel, Kirkby, *et al*, 2001; Hopmans & Bristow, 2002: 71, 121).

Secondly, the cytoplasm of neighbouring cells are connected by tiny channels known as plasmodesmata (Mengel, Kirkby, *et al*, 2001: 113). These are channels that traverse the cell wall to connect the cytoplasm of neighbouring cells and they tend to measure 50 nm or less in size (Peters *et al*, 2021). They allow for the exchange of solutes between neighbouring cells without having to incur the metabolic expense of having to transport them across cell membranes. In the same way that the continuous connection of the cell walls is known as the apoplast, the continuous connection of the cellular cytoplasms is known as the symplasm (Mengel, Kirkby, *et al*, 2001: 113). Figure 4 provides a visual aid for how the apoplast and symplasm look in the broader structure of plant matter.

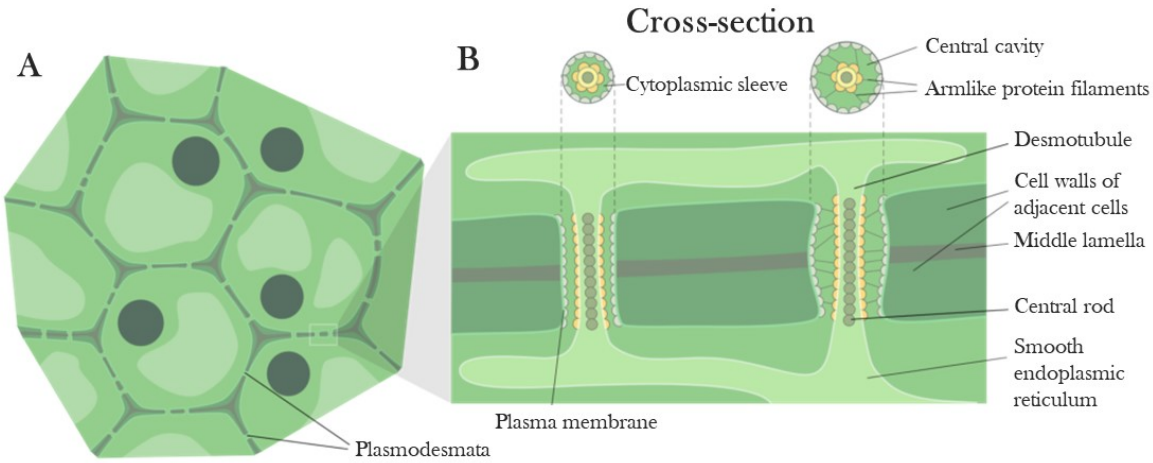


**Figure 4:** View of a collection of interconnected cells. The very dark green circles are the nuclei, the dark green is the apoplast, the light green is the symplasm, and the very light green parts are the vacuoles (adapted from Mokobi (2022)).

### 2.1.2 Overall layout

Plants consist of an above ground part and a below ground part: the superstructure and the root system (Hillel, 2003: 372). The roots are responsible for the absorption of water and nutrients from the soil, as well as the anchorage of the superstructure (Hillel, 2003: 372). Meanwhile, the superstructure hosts the plant's leaves which absorb $CO_2$ and sunlight and use it to manufacture organic products like glucose through photosynthesis (Hillel, 2003: 373). These organic products can then make their way down the stem through the phloem to supply the roots while water and nutrients absorbed by the roots from the soil travel in the opposite direction up the stem through the xylem to the leaves (Hillel, 2003: 373).

Although the exact layout of the roots and the vessels that transport organic products, water, and nutrients varies between dicotyledonous and monocotyledonous roots, the general structure is essentially the same (Kirkham, 2004; Hopmans & Bristow, 2002: 209).

### 2.1.3 Roots and the vascular system

Considering that plant roots are the organs through which nutrients are absorbed, it is important to understand their layout and how they work. The discussion has been divided into a description of the cross sectional and longitudinal structure of the roots.

This is followed by an analysis of the path water and solutes follow from the soil, through the roots, to the xylem.

The cross section of the root consists of concentric rings of different tissue types. Although the exact arrangement depends on the species of plant and whether it is monocotyledonous or dicotyledonous (Kirkham, 2004: 209), the general layout is almost always the same, as outlined in Figure 5.

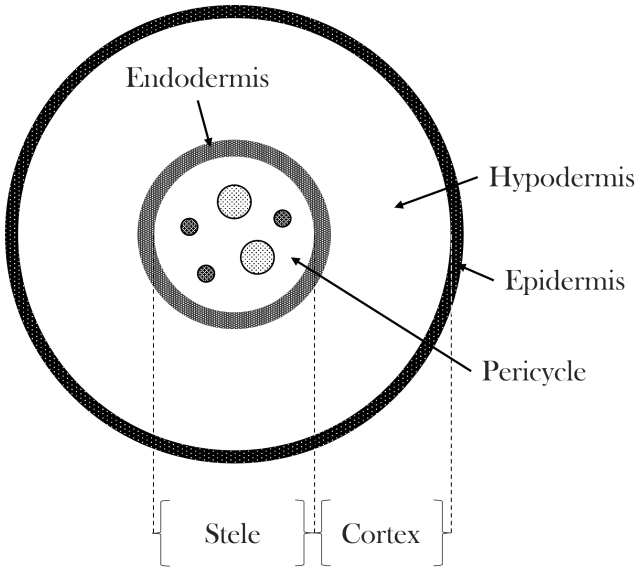


**Figure 5:** Simplified cross-section of the root (adapted from Hopmans & Bristow (2002)).

There are two parts to the root; the stele and the cortex. The stele contains the xylem and phloem vessels, as well as the parenchyma tissue in which these two vessels are embedded. The cortex consists of the endodermis, the hypodermis, and the epidermis. The endodermis demarcates the boundary between the stele and the cortex. Water and nutrients flow through the cortex and cross the endodermis into the stele, from where they are swept up the xylem vessels to the rest of the plant.

The outermost layer is the epidermis. This consists of thin walled, tightly packed cells that can elongate, forming root hairs. These root hairs substantially increase the total surface area of the root and can probe into pores in the soil that the actual root may be too large to reach. This has the effect of increasing water and ion uptake (Kramer, 1983: 120–121). The root hairs on older roots can be destroyed following a deposition of suberin in the epidermal cells, rendering that segment of root much less amenable to water and solute transport (Kramer, 1983: 121).

The hypodermis appears to consist of normal plant cells as described in Section 2.1.1. Root hairs may extend from cells in the hypodermis, through the epidermis (Kramer, 1983: 121).

The endodermis represents the boundary between the cortex and the stele. It is easily recognisable in most plants due to deposits of hydrophobic suberin (a complex organic material) in the apoplast of a single layer of cells, forming a ring around the stele (Hopmans & Bristow, 2002). This suberised layer is known as the Casparian strip and it creates an effective barrier that prevents apoplastic flow from the cortex to the stele. Virtually everything that is exchanged between the cortex and the stele must therefore cross the plasmalemma and follow the syplastic pathway across the endodermis (Hopmans & Bristow, 2002).

Having considered the cross sectional layout of the root, it is now necessary to look at the longitudinal layout of the root. This consists of four sections. The first, at the tip of the root, is the root cap. This consists of clearly defined, loosely arranged cells. It has a mucilaginous consistency that may help ease the movement of the root through the growing medium. Owing to the lack of any vascular structures, it appears to play no part in the absorption of water or nutrients from the soil (Hillel, 2003; Kirkham, 2004: 372, 207).

Following the root cap is the apical meristem, or meristematic region. This region is defined by small, thin walled, tightly packed cells which divide rapidly. It plays little part in water and nutrient absorption from the soil due to the absence of a conducting system and the fact that the cytoplasm in its cells provides significant resistance to the movement of water and salts (Hillel, 2003; Kirkham, 2004: 372, 207).

Behind the meristem there is a region of cell elongation. This consists of cells that elongate along the axis of the root, propelling it forward into the soil. The phloem and xylem vessels start becoming visible in this region (with the phloem being more prominent at this stage). Due to the expression of some cell differentiation, it is difficult to define an absolute boundary between this region and other regions (Hillel, 2003; Kirkham, 2004: 372, 207).

The final region is that of cell differentiation. This is the business end of the root where different cell types and structures are visible and where the bulk of water and nutrient absorption takes place (Hillel, 2003; Kirkham, 2004: 372, 207). Naturally this region represents the bulk of the length of a root, while the other three regions are simply growth phases. Further up the root (closer to the plant crown) the older sections of the roots converge and become increasingly stem-like. At this point they become less absorbent (Hillel, 2003: 373). Moreover, between 1 and 20 cm behind the root tip a secondary deposition of suberin occurs in the epidermis, rendering the root virtually impermeable to solute transport. Hence, it is believed that most water absorption occurs just behind the root tip, though there is evidence that regions of unsuberised epidermis exist further

up the root (Hopmans & Bristow, 2002).

Figure 6 lends a visual representation to the above description.

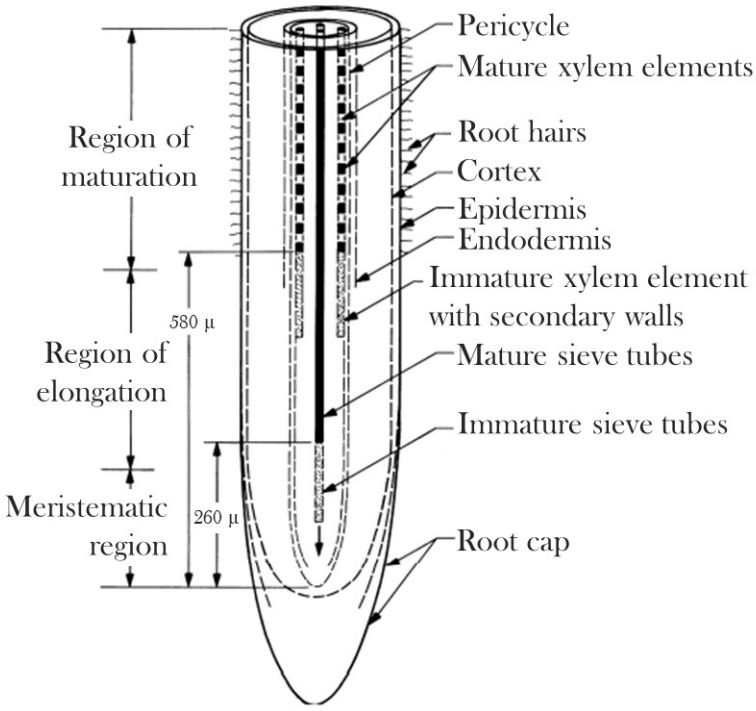


**Figure 6:** Longitudinal section of the root (adapted from Kramer (1983: 123)).

### 2.1.4 Water uptake in plants

Having outlined the physiology of the plant, it is now possible to talk about the mechanisms that drive nutrient uptake.

However, before discussing nutrient uptake mechanisms directly we must consider how water flows through the roots and into the xylem, from where it travels onwards to the rest of the plant. Although nutrient transport across cell membranes is essentially independent of the rate of water flow (Mengel, Kirkby, *et al*, 2001: 186), it remains important to understand how water moves through the plant because nutrient uptake pathways are intimately linked to the movement of water through the plant as whole. After all, the nutrients are dissolved in water, and must therefore traverse the same path through the root that water does.

The driver of all water movement in plants is a property known as water potential (Mengel, Kirkby, *et al*, 2001: 184). Water potential (the chemical potential of water) is defined as the free energy status of water and is taken as the difference in chemical potential of water (J/mol) per unit volume ($J/m^3$) between a water sample and pure, free water at

ambient conditions of temperature and pressure (Mengel, Kirkby, *et al*, 2001: 182–183). Rearranging the units gives a unit of Pa for water potential. Because water potentials are often very large, units of MPa are more often applied (Mengel, Kirkby, *et al*, 2001: 182). Put into layman's terms, water potential is a measure of how freely water molecules can move around (*i.e.* by Brownian motion). If water molecules are more able to move (or move around faster), then the water potential is high. If the movement of the water molecules is constrained, then the water potential is low. As such, water potential is defined by Equation 1.

$$\Psi = \psi_{\mathrm{P}} + \psi_{\mathrm{S}} + \psi_{\mathrm{M}} \tag{1}$$

where $\Psi$ is the water potential, $\psi_{\mathrm{P}}$ is the contribution of water pressure to water potential, $\psi_{\mathrm{S}}$ is the contribution of solutes to water potential, and $\psi_{\mathrm{M}}$ is the matrix contribution to water potential.

$\psi_{\mathrm{P}}$ is numerically equal to the hydrostatic pressure of the solution (Mengel, Kirkby, *et al*, 2001: 183). If the pressure is higher, the water molecules are more energised because they are moving at the same speed as at lower pressure, but they are closer together. Hence, the energy density is higher in a solution under pressure. As such, higher hydrostatic pressures contribute to a positive $\psi_{\mathrm{P}}$, increasing $\Psi$.

$\psi_{\mathrm{S}}$ and $\psi_{\mathrm{M}}$ operate on the general principle that when water adsorbs to a surface, it becomes less mobile (Mengel, Kirkby, *et al*, 2001: 183). Because they are less mobile, they have less energy. The key difference between $\psi_{\mathrm{S}}$ and $\psi_{\mathrm{M}}$ is the type of surface that the water molecule adsorbs to.

Water molecules can adsorb onto macroscopic surfaces (like soil particles, plant roots, the apoplast, etc), immobilising them. When this happens the water potential decreases because the water molecules are less free to move around. This is known as matrix potential, $\psi_{\mathrm{M}}$. The effect of this is that water potentials in soil and the apoplast are always negative.

Similarly, when a solute is introduced, water molecules will also adsorb onto the micro-surfaces of the solute (the solute can be an organic molecule, inorganic ion, etc). This immobilises the water, decreasing its freedom of movement and subsequently decreasing water potential. The contribution of this effect to $\Psi$ is known as solute potential, $\psi_{\mathrm{S}}$. Solute potential is also known as osmotic pressure; the amount of force (*i.e* pressure) applied to a solution to prevent the movement of solvent molecules from pure solvent to the solution across a semi-permeable membrane (Ricca *et al*, 2012; The Editors of Encyclopaedia Britannica, 2023).

Water will flow freely from a region of high water potential to low water potential (*i.e.* from positive water potential to negative water potential, or from negative water potential to even more negative water potential) (Hillel, 2003: 367).

Osmosis refers to the diffusion of water across membranes (Mengel, Kirkby, *et al*, 2001: 185). Osmosis happens when two solutions of differing $\Psi$ are separated by a semi-permeable membrane that allows water molecules to pass through, but not solutes. In plants it is believed that water transport through cell membranes is facilitated by membrane proteins called aquaporins. These allow water molecules to rapidly cross the cell membrane, while remaining impermeable to other ions and solutes (Rubenstein, Yin & Frame, 2021: 430–432). It is speculated that small, polar molecules like ammonia can diffuse through aquaporins as well (AJ Miller & Cramer, 2004). A depiction of an aquaporin is given in Figure 7.

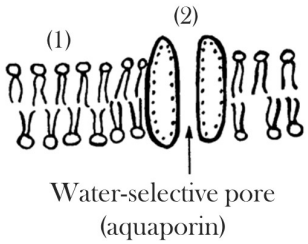


**Figure 7:** An aquaporin situated in the cell membrane. (1) is the cell membrane – comprised of a phospholipid double layer, (2) is the aquaporin protein through which the water molecules pass to bypass the cell membrane (adapted from Mengel, Kirkby, *et al* (2001: 187)).

To understand how this actually works, consider the following example from Mengel, Kirkby, *et al* (2001: 185–187). Two solution, one being pure water and the other solution being a 1 M sugar solution, are separated by a semi-permeable membrane. Each solution occupies a space of 1 L and the container is rigid, preventing expansion. In the sucrose solution, the water molecules are less able to move around because some are bound to the sucrose molecules, decreasing the water potential of the sucrose solution. As a result, the rate at which water molecules collide with (and thus pass through) the semi-permeable membrane is higher on the pure water side. This results in a net flux of water molecules from the pure water to the sucrose solution. Because the volumes are constant, the hydrostatic pressure on either side of the membrane changes. The pressure increases in the sucrose solution while the pressure decreases in the pure water, increasing and decreasing the water potentials, respectively. Eventually, the water potentials of the two solutions will become equal as the collision rate of water molecules with the membrane will be the same on both sides. The end result will be that the sucrose solution will suffer

a much high hydrostatic pressure in order to compensate for the immobilisation of so much of its water content. This phenomena is illustrated in Figure 8.

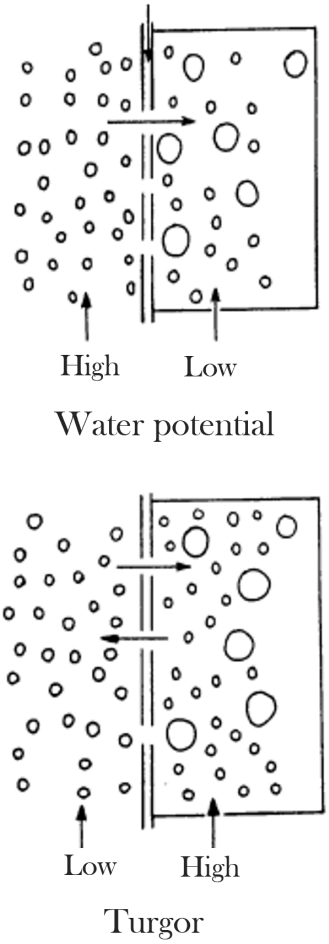


**Figure 8:** The change in water potential of two solutions separated by a semi-permeable membrane. Note how water flows from a high to a low water potential (adapted from Mengel, Kirkby, *et al* (2001: 187)).

This has important implications for the plant cell. The concentration of solutes (ions and inorganic ions) within the cytoplasm of cells is maintained above that of the surrounding soil solution through the action of active ion transport (to be covered in Section 2.1.5) and metabolic production. As such, the cytosol has a negative water potential. This causes water to flow from the surrounding soil into the plant cell, increasing the hydrostatic pressure until the water potential difference becomes zero. As a result, plant cells are rigid due to the turgor pressure this induces. They press against their elastic cell walls, which keep them from bursting, sometimes expanding 20 % to 30 % (Mengel, Kirkby, *et al*, 2001: 186–187).

Now that the principles behind water transport are understood, the means by which plants take up water and transfer it to their leaves can be addressed. Sadly, despite

possessing a greatly expanded knowledge about plant-water relations as compared to 100 years ago, the controversy surrounding water movement between roots and shoots has only intensified in recent years and shows no signs of abating (Tyree, 2003; Bentrup, 2017). The dispute centres on cohesion-tension theory and its role in water transport up the xylem. The cohesion-tension theory states that the evaporation of water from the leaves of a plant pulls water up the xylem to replace the lost water. The water column is therefore under tension as water is pulled from the soil through a continuum of water running from the soil to the leaves (Kirkham, 2004: 203). Although the debate around this remains active (and in some cases acrimonious) the cohesion-tension theory seems the best current explanation for water movement up the xylem.

Although it is now understood to be much more complex (Bentrup, 2017), water flow from the soil to the leaves seems to happen in essentially two regimes: low transpiration and high transpiration (Kirkham, 2004: 170). Regardless of the regime, the water will have to travel axially through the cortex to reach the xylem. There are three ways water can cross the cortex into the stele and on to the xylem: the apoplastic pathway, the symplastic pathway, or by alternating between the two - crossing the symplasm of one cell before being disgorged into the apoplast and re-entering the symplasm of the next cell on the way to the stele. Ultimately, however, the water must cross the Casparian strip, necessitating the symplastic route for at least part of the journey (Mengel, Kirkby, *et al*, 2001: 194). Figure 9 shows the different path through the roots to the xylem.

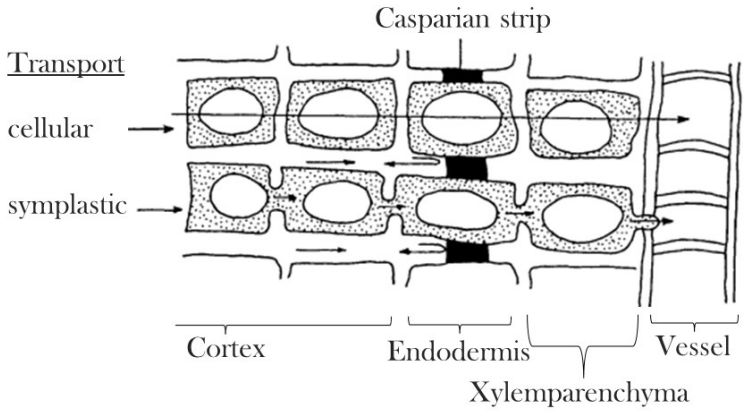


**Figure 9:** The route of water through the cortex to the xylem vessels. Note how the apoplastic route is cut off by the Casparian strip (adapted from Mengel, Kirkby, *et al* (2001: 194)).

Once in the stele, water travels up the xylem to reach the leaves and then diffuses through the stomata to cross from the leaves to the air. This is known as the soil-plant-air-continuum, or SPAC. The SPAC is illustrated in Figure 10.

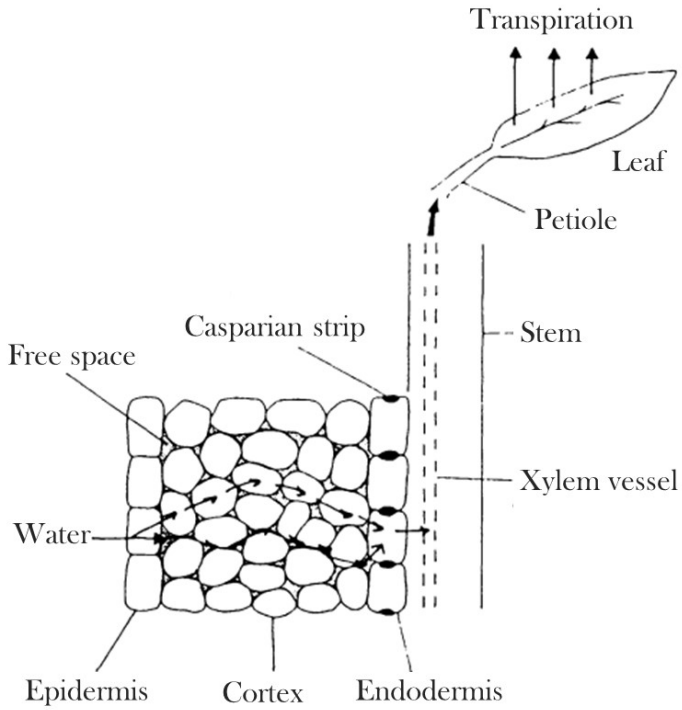


**Figure 10:** The SPAC: the continuum of water stretching from the soil to the leaves (adapted from Mengel, Kirkby, *et al* (2001: 190)).

The first regime, known as bulk flow, is the simplest to understand and for much of the twentieth century was believed to be the only cause of movement between roots and shoots (Bentrup, 2017). In instances of high transpiration rates, water evaporates rapidly from the leaves. This generates a large negative pressure within the leaves, pulling water from the xylem to replace the lost water. This high negative pressure is transmitted down the xylem to the roots and then to the soil. The water-continuum within the plant is kept intact by the cohesion between water molecules, creating a constant flow of water from the soil, through the roots, up the xylem, through the leaves, and into the air (Kirkham, 2004: 168). In this case, water is flowing down a pressure gradient where the negative pressure in the xylem creates the necessary potential gradient to encourage water to leave the relatively saline symplast for the more dilute apoplast (Mengel, Kirkby, *et al*, 2001: 168).

Alternatively, under conditions of low transpiration rates (at night or in high humidity), water is delivered to the xylem by osmosis (Mengel, Kirkby, *et al*, 2001: 195). From there a combination of root pressure and cohesion forces drives the water upwards. This osmotic pathway is driven by water potential. Water diffuses from the soil solution into plant cells. It then travels across the Casparian strip into the stele. Once in the cells of the stele, it diffuses across the cell membranes out of the cell and into the apoplastic space where it joins the xylem. The diffusion out of the plant cells seems to tied to the action

of potassium and chloride pumps in the cell membranes of the stele (Bentrup, 2017). Solutes are pumped into the xylem, lowering the water potential and prompting water to diffuse out of the symplasm to the xylem. Because the xylem is so large and because it is essentially open to the atmosphere (because of the leaves and their stomata), this influx of water does not increase the hydrostatic pressure of the xylem. Instead it pushes the water upwards towards the leaves. This causes positive root pressure and is responsible for guttation (the exudation of water from leaves) (Mengel, Kirkby, *et al*, 2001: 199).

Regardless of the means by which water enters the xylem, it is believed that transpiration is what often drives the movement of water up the xylem to the leaves. This is because root pressures are generally not large enough to move water the great heights (up to 100 m) needed in larger plants like trees (Mengel, Kirkby, *et al*, 2001: 200).

### 2.1.5 Nutrient uptake mechanisms

Much like the movement of water described above, the path of nutrient entry into the plant has three phases. The first is the movement of nutrient ions to the root surface. The second is the movement of these nutrients across the cortex and into the stele (Kramer & Boyer, 1995: 288). Finally. the third is the dumping of nutrients into the xylem, up which they travel to the rest of the plant (Kramer & Boyer, 1995: 186). Each of these will be dealt with in turn.

The first phase, movement of nutrients to root cells is relatively simple to understand. Nutrients are brought to the root surface by two means; bulk flow and diffusion (Barber, 1962). Bulk flow refers to the movement of nutrients carried by the transpiration stream. In periods of low transpiration, bulk flow fails to deliver nutrients to the cell membrane as fast as they are absorbed. This leads to a concentration gradient developing between the cellular surface and the bulk solution as ions are taken up by the plant faster than they are supplied by bulk flow. As a result of this concentration gradient, nutrients will diffuse from the bulk solution to the root surface, increasing the supply of nutrients above that which can be expected from bulk flow alone (Kramer & Boyer, 1995: 287).

Conversely, if transpiration is high enough, then nutrients are delivered to the root surface faster than they can be absorbed, leading to a build-up of nutrients at the root surface. This results in back diffusion from the root surface to the bulk solution (Kramer & Boyer, 1995: 287)

In any case, once on the root surface the nutrients face a choice: they can travel through the cortex via the apoplatic pathway or the symplastic pathway (Hopmans & Bristow,

2002). Because soil solution travels freely within the apoplast, some nutrients will go this route, though as long as nutrients are adjacent to cell membranes, they are liable to enter the symplasm. Thus the exact path is not important. What is important is that eventually nutrients will be forced to enter the symplastic route in order to cross the Casparian strip in order to reach the xylem (Hopmans & Bristow, 2002). It is true that in young, unsuberised roots that nutrients can simply join the bulk flow of water through the roots to the xylem (Hopmans & Bristow, 2002). However, this does not represent a major pathway for nutrient transport.

It is important to note that the movement of ions to the root surface is neither limiting, nor is it very selective. It is not selective because bulk flow simply carries the ions to the root surface in the same ratio that they occur in the solution. It is not usually limiting (at least in the case of nitrate) because nitrate uptake rates have been found to be independent of transpiration rate. Only at low transpiration rates has nitrate uptake rate seen to be inhibited. However, this has been attributed to the build-up of nitrate in the xylem which inhibits the metabolically driven transport of nitrate into the xylem from the cells of the parenchyma (Hopmans & Bristow, 2002; Shaner & S, 1976). As such, it is not the reduction in ion transport to the roots that one would expect from reduced bulk flow, but the sluggish pace of ion transport away from the roots up the xylem, that causes reduced nitrate uptake. This implies that diffusion through the solution makes up for any shortfall in nutrient supplies to the roots. As such, the rate of transport across the plasmalemma is what determines the rate of nutrient uptake.

Mirroring the path that water follows through the roots, there are two paths that nutrients can follow through the cortex: the apoplastic and/or symplastic routes (Hopmans & Bristow, 2002; Barberon & Geldner, 2014). The existence of a third pathway has been proposed by Barberon & Geldner (2014). This is called the coupled trans-cellular pathway and involves the movement of nutrients from cell-to-cell by influx/efflux transporters on cells. The theory is that influx and efflux transporters are polar and occur opposite one another and thus form a directional route from the hypodermis to the xylem vessel. Admittedly, its not a given that this actually happens, though both apoplastic and symplastic flow are widely acknowledged to exist. Figure 11 illustrates the three pathways through the cortex.

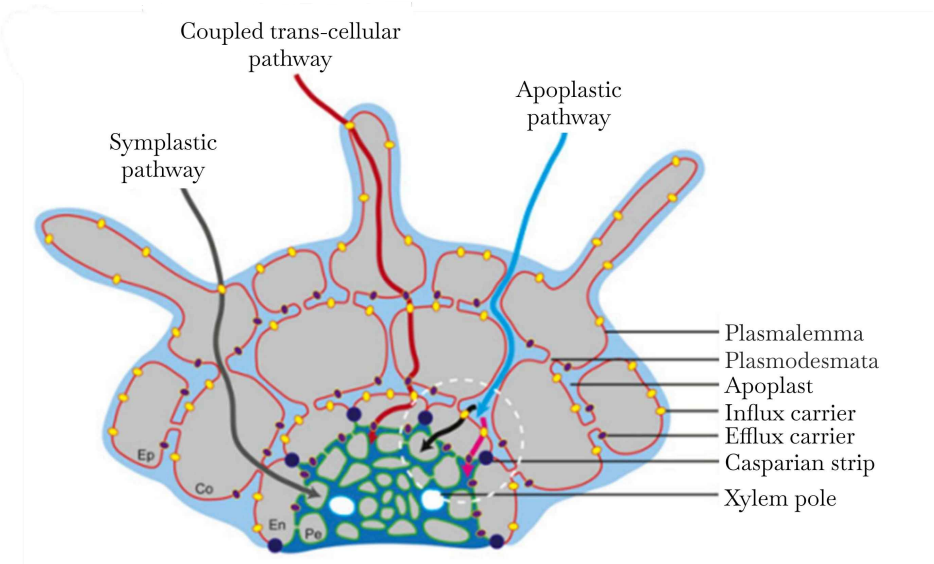


**Figure 11:** The three pathways down which nutrients can travel through the cortex (adapted from Barberon & Geldner (2014)).

Just as in the case with water movement, the flow of nutrients is impeded by the presence of the Casparian strip. At this point all nutrients travelling to the xylem must cross into the symplasm in order to bypass the Casparian strip (Barberon & Geldner, 2014). This involves the crossing of cell membranes, after which nutrients can simply travel through the plasmodesmata connecting the neighbouring cells before being dumped in the apoplast of the stele. As such, regardless of the path followed, nutrients must cross the plasmalemma, making understanding cross-membrane transport fundamentally important to understanding nutrient transport.

Ion transport across the plasmalemma can be achieved through two means: ion channels and carrier proteins (Hopmans & Bristow, 2002). Ion channel transport can further be broken down into three mechanisms: facilitated diffusion (symport or uniport), cotransport, and antiport (Mengel, Kirkby, *et al*, 2001: 128). The general idea of symport, cotransport, and antiport is conveyed in Figure 12.

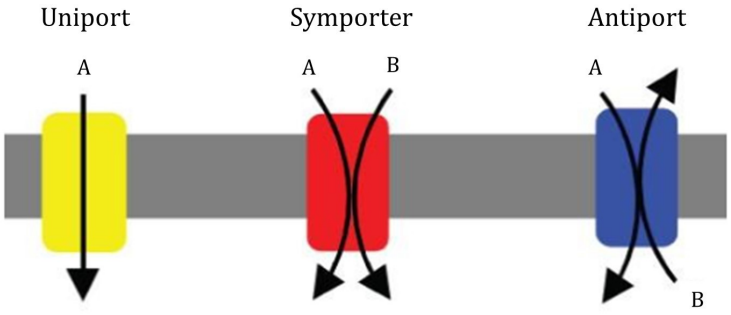


**Figure 12:** From left to right: uniport, cotrasport, and antiport (Mattaini, 2020: 288).

All three ion channel methods rely on the actions of ion pumps, in particular the $H^+$-ATPase transporter that pumps protons from the cytosol into the apoplast (Mengel, Kirkby, *et al*, 2001: 118), a diagram of which is shown in Figure 13.

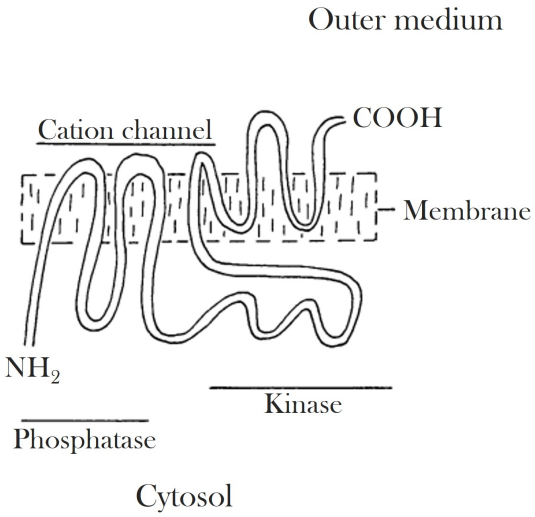


**Figure 13:** A proton pump embedded in the plasmalemma (adapted from Mengel, Kirkby, *et al* (2001: 118)).

By constantly pumping protons out of the cytosol, the cell interior gains a negative charge relative to the rhizosphere. This creates an electrochemical gradient across which cations like $NH_4^+$ may flow. The flow of these ions through the ion channels is referred to as facilitated diffusion because their flow into the cell has been facilitated by providing an electrochemical gradient that overcomes the chemical potential of the cations (Mengel, Kirkby, *et al*, 2001: 120).

Cotransport (or symport) happens for exactly the same reason, but involves the movement of anions (Hopmans & Bristow, 2002). Anions are negatively charged, and thus are repelled by the negative cell interior. Their movement into the cell is facilitated by the formation of complexes with protons, giving the anion complex a net positive charge (*i.e.*

in order to move nitrate through cotransport, two protons are needed; one to nullify the negative charge and one to create the net positive charge) (Mengel, Kirkby, *et al*, 2001: 126). This is in fact how nitrate transport is believed to occur (Hopmans & Bristow, 2002). Interestingly, cotransport also plays a major role in moving some cations, specifically $K^+$ and is particularly important in low $K^+$ environments (Mengel, Kirkby, *et al*, 2001: 127–128). Literature reveals that the apoplast typically has a lower pH than the symplasm with pH ranges for the two typically being 4.9 to 5.8 and 7.1 to 7.5, respectively (Felle, 2001; Wegner & Shabala, 2019).

Finally there is antiport. This is similar to normal facilitated diffusion, except that it involves the movement of protons into the cytosol and the expulsion of cations. It is important for regulating the concentration of cations in the cytosol and it is believed that this plays an important role in keeping concentrations of Na low by expelling it into the apoplast (Mengel, Kirkby, *et al*, 2001: 128).

These three channel transport methods are illustrated in Figure 14.

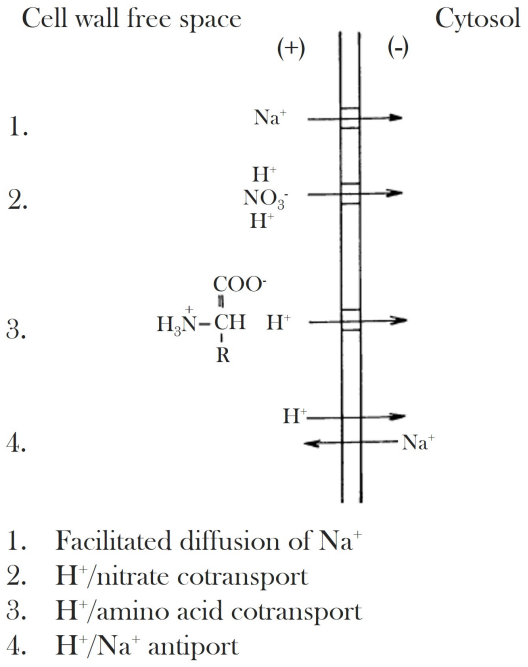


**Figure 14:** The three means by which nutrients move through ion channels. Note that all of them are dependent on proton pumping and that (2) and (3) represent the same process (cotransport) but with different molecules complexed to $H^+$ (adapted from Mengel, Kirkby, *et al* (2001: 127)).

Generally these channels are selective, but it is not clear how selective. It is known that $NH_4^+$ can move through $K^+$ channels, though the channel remains more partial to $K^+$ (Mengel, Kirkby, *et al*, 2001: 127). It is possible that the selectivity of the channels (at

least in part) relies on the fact that they close when cytosolic concentrations exceed a given value, diminishing the movement of a particular ion (Mengel, Kirkby, *et al*, 2001: 124). It is also important to note that, although often classified as passive transport, the fact is that energy must be expended to create the electrochemical gradient down which these ions move, making channel transport active (Hopmans & Bristow, 2002).

Carrier proteins function on a different basis to ion channels. Instead of allowing a path for ions to diffuse through the plasmalemma, the protein itself diffuses through the membrane where it attaches to the desired nutrient and then transports it to the other side of the plasmalemma (Mengel, Kirkby, *et al*, 2001: 128). These are believed to be much more selective, but also much slower than ion channels (Hopmans & Bristow, 2002); some estimates put ion channel diffusion at 100 to 1000 times faster than carrier transport (Hedrich & Schroeder, 1989). As such, whereas it was previously believed that carrier transport used to play an important role in nutrient transport, it is now believed that the bulk of nutrient movement is achieved by ion channels (Mengel, Kirkby, *et al*, 2001: 128). Figure 15 illustrates how carrier transporters are believed to work.

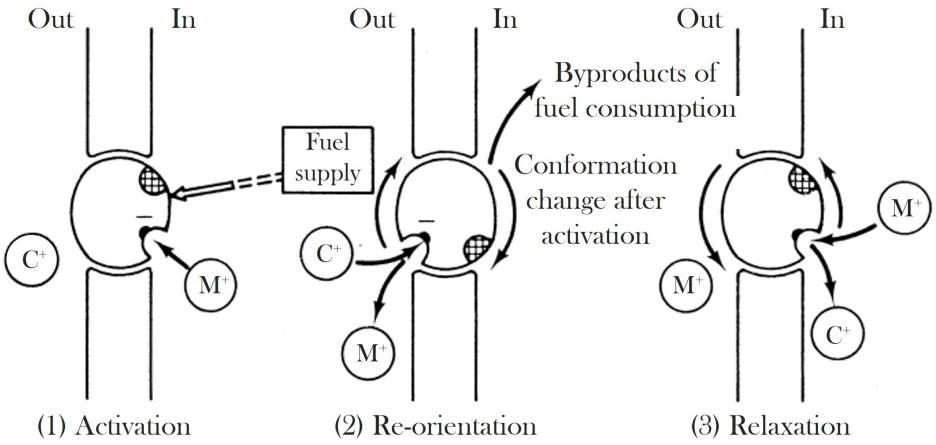


**Figure 15:** Carrier protein exchanging ions between the symplast an apoplast (adapted from Clark (1974) cited by Hopmans & Bristow (2002)).

It is commonly understood in literature that ion channels and carriers drive two different mechanisms: the low affinity transport (LATs) and high affinity transport (HATs) (Hopmans & Bristow, 2002), respectively. The theory states that the high selectivity of the carrier transporter makes it more effective at lower concentrations than the ion channels, meaning that two different mechanisms exist at different concentrations. To put the difference in regime into perspective, the HATs regime for nitrate only becomes dominant at $NO_3^-$ cncentrations below 0.5 mM (Glass & Siddiqi, 1995). However, it is important to note that the idea that two different mechanisms are operating simultaneously has come under sustained attack over the years (Dreyer & Michard, 2020; Dalton, 1984). The key

issue raised by Dreyer & Michard (2020) is that nutrient uptake kinetics are typically modelled as enzymes using Michaelis-Michelin kinetics. Although this gives a good fit to data, it is physically misleading as to how ions are actually transported within plant cells. Thus, although the mechanisms differ in terms of the amount of material they transport, and the selectivity with which they do so, it may not be wise to assume that one dominates in a particular concentration regime.

Different transport channels and carriers (both being proteins) are coded for in DNA (Masclaux-Daubresse *et al*, 2010), with many different transporter genes across many different species having been identified. This provides the physiological basis for the inane preference of plants for ammonium or nitrate because both rely on (relatively) ion-specific channels. Certain species like rice simply have more genes pertaining to ammonium transport than nitrate transport (and vice versa for nitrate loving plants), owing to the fact that rice has evolved to live in an ammonium rich environment (Masclaux-Daubresse *et al*, 2010) (this is expounded upon in Section 2.2.1). However, it must be noted that if demand for nutrients is high, genes can be upregulated to meet it, possibly explaining how nitrogen uptake can remain constant across different ammonium/nitrate regimes (Mengel, Kirkby, *et al*, 2001: 136). This means that as demand for nitrogen increases, genetic traits pertaining to ion transport will be made more prominent, such that increasing amounts of available nitrogen forms can be transported.

Once past the Casparian strip, the nutrients need only diffuse out of the symplast into the apoplast, through which they will join a xylem vessel that will transport them up the stem to the leaves in the bulk flow of water upwards (Mengel, Kirkby, *et al*, 2001: 207). Movement of nutrients from the cells of the stele into the xylem seems to occur by much the same process that absorption does: ion channels and carriers. Hence, it remains under tight metabolic control, just like nutrient absorption (Mengel, Kirkby, *et al*, 2001: 197).

It is important to note that the roots are also a centre of metabolic activity where many organic molecules are synthesised and then transported from the roots. As such, amino acids are also dumped into the xylem for transport to the leaves, meaning some of the ammonium and nitrate absorbed by leaves is processed before reaching the xylem (AJ Miller & Cramer, 2004). In particular, it is believed that much of the ammonium is utilised in the roots to manufacture amino acids (Patterson *et al*, 2010), though under pure ammonium nutrition ammonium is liable to diffuse into the xylem and travel up to the leaves (Mengel, Robin & Sal sac, 1983: 210).

Thus far nutrient transport has been discussed as a largely active phenomenon. This means that energy is expended by the plant to move the nutrients from the soil solution to

the xylem. The reason for this is that the vast majority of ions that enter the xylem must pass through the Casparian strip, and to pass through the Casparian strip they must cross the plasmalemma. As has been discussed earlier, crossing the plasmalemma is mediated by various carrier proteins which require energy to work, making cross-plasmalemma transport an active phenomenon.

However, transport that does not require energy input from the plant is also possible. This is called passive transport and tends to involve the flow of ions along concentration gradients or nutrients being swept into the xylem by the bulk flow of water from the soil (Hopmans & Bristow, 2002: 132). Xiaochuang *et al* (2015) analysed the fraction of N taken up by pakchoi plants through active and passive transport and found that at low N concentrations (0.025 mM N) active uptake accounted for roughly 90 % of N uptake while at high N concentrations (1.5 mM) active uptake accounted for between 70 and 80 % of N uptake. Thus, despite active transport (which is selective) representing the bulk of N absorption, it is important to remember that any uptake ratio between ammonium and nitrate will be influenced by the non-selective passive uptake mechanism.

### 2.1.6 Implications for pH

Regardless of the exact means by which nutrients are transported across the cell membrane, it is widely acknowledged that ion pumps (specifically proton pumps), have a lot to do with it. The activity of $H^+$-ATPase and costransport have profound implications for the pH of the rhizosphere. The absorption of $NH_4^+$ drives pH downward as protons must be pumped out of the cell in order to maintain the electropotential gradient. Conversely, because the uptake of $NO_3^-$ takes place by cotransport, whereby each $NO_3^-$ must be accompanied by at least one proton, the net effect is an increase in rhizosphere pH as the rhizosphere is drained of protons. In a system where both are present, the pH change is reduced because protons expelled by the proton pump are brought back in by $NO_3^-$ cotransport. This was proven in a study by Ismande (1986) whereby soybean plants were fed mixtures of ammonium and nitrate at different ratios.

However, this begs the question: what ratio of ammonium-to-nitrate is needed to maintain pH? Raven (1985) found that, generally speaking, every mole of ammonium taken up released 4/3 mol of protons while every mole of nitrate absorbed produced 2/3 mol of hydroxide ions. However, this refers to pure ammonium/nitrate, and does not account for the pH effect of absorbing all the other anions and cations needed by plants. Moreover, different plants will show different ratios. Ismande (1986) found that the ratio of ammonium-to-nitrate needed to maintain pH homeostasis after nitrogen depletion was

one to four for soybeans, which is clearly different to the one to two ratio resultant from the findings of Raven (1985).

More importantly, the numbers of protons released by *B. oleracea* var. *acephala* per mole of ammonium and absorbed per mole of nitrate were found by van Rooyen & Nicol (2021) to be 1.0 and 0.5, respectively. This was calculated from experiments that used nitrogen in Hoagland solution. As such, these figures not only take into account the inane preference of the plant used in this study, they also capture the effect that other nutrients would have on the proton/hydroxide ratios of ammonium/nitrate absorption.

This would suggest that in order to maintain a constant pH, ammonium and nitrate must be absorbed in a ratio of one to two. Although it is tempting to say that this can be achieved by supplying the plants with a nutrient solution of the same ratio, it is not so simple. Firstly, uptake ratio is related to concentration ratio, but it is not equal to concentration ratio. This shall be expounded upon in Section 2.1.7. Secondly, the natural variation of plants in the rate and ratio that they absorb nutrients (as discussed before) is such that a one-size-fits-all nutrient solution and dosing solution would lead to a gradual deterioration in the pH over time. This necessitates the use of the active control system posited in this study.

### 2.1.7 Relationship between uptake rate and concentration in the nutrient solution

Having looked at the broad swathe of nutrient absorption and movement within plants, the relationship between uptake rate and concentration must now be discussed. It is clear that most nutrient absorption is facilitated by partially selective ion channels with lesser contributions from non-selective passive transport and hyper-selective carrier-based transport exists. Thus, nutrient uptake is a largely selective process with the exact ratio being a function of the preference of the plant. However, studies have found there to be correlation between uptake rate and concentration in the nutrient solution. As stated earlier, these are often quantified using Michaelis-Menten kinetics

$$V_i = V_{max} \frac{C_i}{C_i + K_m} \tag{2}$$

where $V_i$ is the uptake rate ($\mu$mol per g fresh root mass per hour) of chemical species $i$ at concentration $C_i$ (mmol/L). $V_{max}$ is the maximum uptake rate ($\mu$mol per g fresh root mass per hour) and $K_m$ is the half-saturation constant (mmol/L). Although Michaelis-Menten kinetics provide a good fit to data and thus can be used for modelling, caution

must be exercised when trying to assign physical significance to the parameters (Dreyer & Michard, 2020).

Because nitrogen represents the bulk of ions absorbed by plants, this discussion will focus on the uptake kinetics of nitrogenous species, specifically ammonium and nitrate.

Most studies reviewed regarding the relationship of ammonium and nitrate concentrations in the nutrient solution with plants dwelt on the effect that they have on growth (Song, L Li, *et al*, 2017; Wang *et al*, 2022; Wenceslau *et al*, 2021; Lobit *et al*, 2007), with a lesser portion investigating the kinetics of nitrate and ammonium uptake (Song, G Li, *et al*, 2016; Wang *et al*, 2022). Moreover, both of these studies deal with *Brassica oleraceae* var. *alboglabra*, not *B. oleraceae* var. *acephala*, as is the object of the investigation. Thus any cross comparison must be made with caution.

Song, G Li, *et al* (2016) applied a nutrient depletion technique to the plants over 5 hours by placing plants in 50 mL of different nitrogen solutions and measuring the beginning and end concentrations and volumes. From this they reached the conclusion that nitrate was indeed the preferred nitrogen source. The results generated by Wang *et al* (2022) tell a similar story with nitrogen depleting faster than ammonium, even in high ammonium systems.

As the most complete kinetics for ammonium and nitrate uptake by a *B. oleraceae* variety, the Michaelis-Menten kinetic parameters proposed by Song, G Li, *et al* (2016) will be used. These are presented in Figure 16. Not only are ammonium and nitrate uptake rates presented, but Figure 16 shows the uptake rates of various other nitrogen forms as concentration changes for Chinese kale.

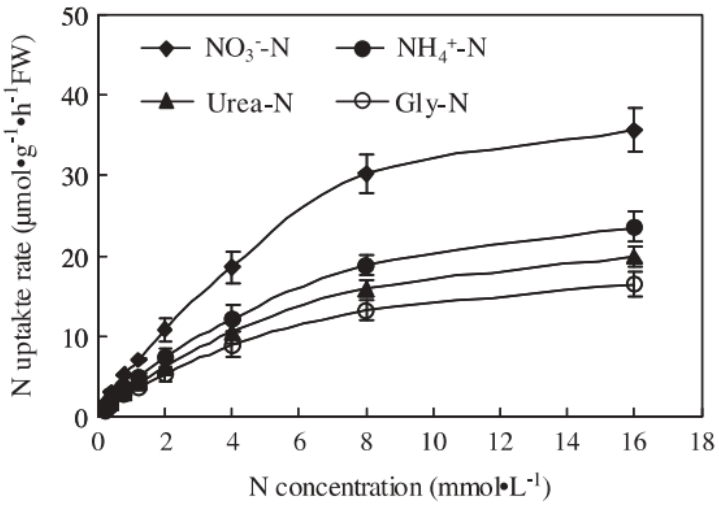


**Figure 16:** Comparison of the uptake rates of different nitrogen containing species (Song, G Li, *et al*, 2016). Gly refers to the amino acid, glycine.

As can be seen, there is a clear relationship between concentration and uptake rate. This makes perfect sense as it stands to reason that as the concentration in the nutrient solution increases, the chance of a molecule diffusing from the apoplast into the root increases.

There is also a clear tendency of the plant to favour certain nitrate sources above others. In this case, the plant appears able to absorb inorganic nitrogen (specifically nitrate) faster than organics like glycine and urea.

### 2.1.8 Summary

In order to enter the xylem (and travel on to the rest of the plant) nutrients must cross the Casparian strip. In mature roots this can only be achieved by crossing the plasmalemma into the symplasm, after which the nutrients cross the plasmalemma into the apoplast of the stele, joining the xylem. There are multiple mechanisms by which this is achieved, with the most important being ionic movement through ion channels. This makes nutrient uptake an inherently selective process

Anionic $NO_3^-$ is mostly taken up by cotransport (Ullrich, 1992), leading to a pH rise in the medium. Cationic ammonium is mostly taken up by diffusion down the electrochemical gradient created by the action of proton pumping. The cultivation of plants in pure solutions of either will knock the pH off kilter, necessitating pH control.

It must also be understood that ion uptake rate is related to the growth rate of the plant and its physiological requirements (Mengel, Kirkby, *et al*, 2001: 135) and not completely by the nutrient content of the medium. In fact, nutrient uptake is controlled by the concentration of nutrients within the cell (and is thus coupled to growth rate), making uptake rates partially independent of external concentration (Mengel, Robin, *et al*, 1983: 135). However, the experiments on Song, G Li, *et al* (2016) and Xiaochuang *et al* (2015) show that uptake rate and concentration are related.

Finally, because transporters are coded for in the genetics of a plant, certain plants will be more predisposed to certain combinations of nutrients. However, it is possible that this may change over the life of the plant as the number and nature of transporters within the root adjust to take into account the composition of the nutrient solution (Mengel, Kirkby, *et al*, 2001: 136). Moreover, the presence of limited passive transport systems (particularly at high concentrations) will likely moderate the uptake ratio in the direction of the ammonium/nitrate ratio. Although far from perfect, Michaelis-Menten kinetics represent a convenient way of relating nutrient concentration to nutrient uptake.

## 2.2 Nitrogen nutrition

Having thoroughly addressed the general theory of how plants absorb nutrients and considered the kinetics of nitrogen absorption, it is now necessary to address some of the finer points of nitrogen nutrition that must be considered when growing plants hydroponically.

### 2.2.1 Key nitrogen sources

Nitrogen in the environment is available to plants in three forms: $NH_4^+$, $NO_3^-$, and amino acids (AJ Miller & Cramer, 2004). Plants generally rely on $NH_4^+$ and $NO_3^-$ to supply their nitrogen (AJ Miller & Cramer, 2004), but can also take up amino acids directly, albeit in smaller quantities (AJ Miller & Cramer, 2004; Song, G Li, *et al*, 2016; Zhu *et al*, 2018). As stated in Section 2.1.5 the preference of plants for one or the other is guided by genetics, as well as the concentration in the rhizosphere. The genetic preference is likely a manifestation of the environment where the specific plant originated. Plants adapted to cold or anoxic soils prefer ammonium while plants indigenous to aerobic soils prefer nitrate. This is because in cold or anaerobic soils, nitrification is suppressed, making ammonium the dominant N-faction. Conversely, in warm, aerobic soils nitrification can continue uninhibited, making nitrate the more prevalent N-faction (AJ Miller & Cramer, 2004; Assimakopoulou *et al*, 2019). The preference of plants towards ammonium or nitrate can be thought of as a "continuum" of species ranging between those that like ammonium to those that prefer nitrate, with many plants preferring a combination of the two (AJ Miller & Cramer, 2004). It is important to note that closely related species vary greatly in their response to ammonium concentration (AJ Miller & Cramer, 2004).

In environments where ammonium is prevalent it is advantageous for plants to exploit it. This is because ammonium can be used directly in amino acid synthesis without having to be first reduced like nitrate, making it more energetically favourable (Raven, 1985; Salsac *et al*, 1987). However, when ammonium concentrations are high, this often turns into a case of too much of a good thing. Under ammonium rich conditions, plants will absorb too much ammonium, leading to ammonium toxicity. Ammonium concentrations in the natural environment are usually very small (owing to the action of nitrifying bacteria). As such, plants tend to lack mechanisms that exclude ammonium from their cells because ambient ammonium concentrations are seldom high enough to pose a threat (AJ Miller & Cramer, 2004). The end result is the paradoxical situation where plants may be genetically predisposed to absorbing ammonium, but they cannot be supplied with an ammonium heavy medium in a hydroponic setting because they risk poisoning themselves. Bloom (1988) compared this to the simple analogy of a child being given unlimited candy; eventually the child eats so much that it becomes ill.

### 2.2.2 Effect of nitrate on plants

Nitrate is non-toxic and highly soluble, making it ideal for storage by plants in the vacuoles of their cells. As such, high nitrate fractions in the nutrient solution lead to high nutrient contents in the leaves while replacing some nitrate with ammonium has been proven to reduce nitrate content (Song, L Li, *et al*, 2017; Zhu *et al*, 2018). However, the jury is still out on whether nitrate accumulation is substantial enough to cause concern. From literature it is known that the nitrate content of kale leaves grown in high nitrate hydroponic environments often skirt close to (if not exceed) the limits imposed by food standards agencies like those within the EU (European Commoission, 2023; Fallovo *et al*, 2006; Santamaria, 2006; Song, L Li, *et al*, 2017; Zhang *et al*, 2007). Moreover, although nitrate is carcinogenic (this is, in fact, the primary reason why its content in food is regulated by bodies like the EU; it is associated with stomach cancer as well as methaemoglobinaemia (Ramazzotti *et al*, 2013; Gorenjak & Cencič, 2013)), the consumption of increased amounts of nitrate has been found to correlate with *lower* rates of cancer. This is likely due to the fact that if you consume lots of nitrate, you probably have lots of leafy greens in your diet. The health benefit of these foods serves to offset the threat posed by the high amounts of nitrate they often contain (Santamaria, 2006).

### 2.2.3 Effect of ammonium on plants

Given that sensitivity to ammonium is dependent both on plant species and the ratio of ammonium-to-nitrate, it should come as no surprise that many studies focus on the effect of ammonium-to-nitrate ratio on the growth rate of plants. It is common in work that involves varying the ammonium and nitrate composition to observe reduced growth and other signs of physical distress in plants at high ammonium concentrations and this is no exception for *Brassica oleraceae*. Studies have found that in the early stages of growth that kale shows no negative side-effect from high ammonium concentrations, but prolonged exposure during maturity lead to reduced growth (Wang *et al*, 2022; Assimakopoulou *et al*, 2019).

The literature is somewhat conflicted as to the exact point where yields drop significantly, but experiments by Wang *et al* (2022) on Chinese kale (*B. oleraceae* var. *alboglabra*) suggest that seedling growth was promoted at 50 % $NH_4^+$, but that this fraction ultimately led to inhibited growth in the later stages of the plant's life. Similar experiments by Assimakopoulou *et al* (2019) on *B. oleraceae* var. *acephala* suggested that ammonium concentrations up to 50 % of total N provided acceptable growth rates. It is unclear whether this is a difference between the cultivars or simply a change in the author's

definition of a good growth rate. However, it is clear that high ammonium concentrations and fractions can be problematic.

Optimal growth is typically achieved in a nitrate heavy growth medium in which $NH_4^+$ represents between 10 % and 25 % of total nitrogen content (Assimakopoulou *et al*, 2019; Wang *et al*, 2022), though some literature has also found that, barring ammonium toxicity, that the growth rate remains unchanged with the addition of ammonium (Zhang *et al*, 2007). It must be noted that at constant nitrogen concentration, a higher ammonium fraction would mean a higher absolute ammonium concentration. As such, it may not be prudent to simply declare that a certain nitrate/ammonium ratio is ideal, because if the total nitrogen concentration is sufficiently low, then the ammonium concentration could be low enough to avoid ammonium toxicity, even at high ammonium/nitrate ratios.

Adding ammonium to the growth medium has also been found to have several interesting effects on the nutritional quality of the produce. It has been found to suppress nitrate build-up in the leaves of *B. oleraceae* var. *acephala* while simultaneously encouraging protein synthesis (Zhang *et al*, 2007; Zhu *et al*, 2018). It has also been found in some studies to enhance the concentration of valuable phytochemicals like vitamin C (Zhu *et al*, 2018). However, owing to its positive charge, it jockeys with other cations for entrance into the roots, and as a result has been found to lower the mineral content of the leaves (*i.e* Ca, Mg, K, etc) (Song, G Li, *et al*, 2016).

### 2.2.4 Ammonium toxicity in plants

Given the evident distress that kale experiences in ammonium rich regimes, it is worth considering the mechanisms by which ammonium toxicity actually occurs. Virtually all plants have been seen to exhibit symptoms of ammonium toxicity when exposed to high ammonium concentrations (Britto & Kronzucker, 2002). However, this does not mean to say plants are actually being *poisoned* by ammonium. Ammonium itself is not toxic. Instead it was thought that ammonium breaks down in the plant to ammonia, which *is* toxic (Hu *et al*, 2015; Zhang *et al*, 2007). However, at pH values below 8, ammonia is practically absent, as detailed in Figure 17. Considering that the pH of the cytosol is usually in the range of 7.1 to 7.5 (Felle, 2001; Wegner & Shabala, 2019), there is little possibility that free ammonia is the culprit. Considering that ammonium itself is non-toxic, the accumulation of this in plant cells cannot be singled out as the cause of ammonium toxicity either (Britto & Kronzucker, 2002; AJ Miller & Cramer, 2004).

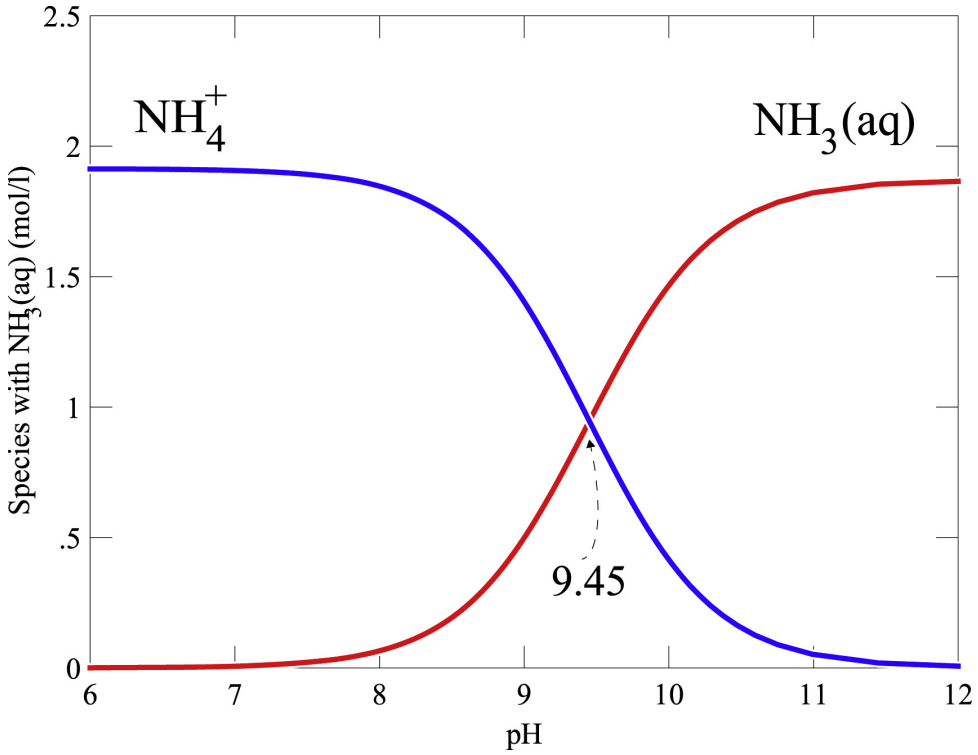


**Figure 17:** Change in form of ammoniacal species with change in pH (Velásquez-Yévenes & Ram, 2022).

As was discussed under Section 2.1.6, ammonium nutrition tends to result in acidification of the root zone. While many plants (including kale) prefer a slightly acidic environment, the extent to which this happens in ammonium rich systems is often extreme, burning plant roots. As a result, simply controlling pH has often been seen to eliminate ammonium toxicity in many plants (Britto & Kronzucker, 2002).

However, this is not guaranteed to eliminate the negative effects of ammonium on plants. Some species do have a genuine toxic response to ammonium. Unfortunately, this seems to be the case with kale. Not only does literature report low growth rates in ammonium rich systems for kale, but *Brassicaceae* are highlighted as an ammonium sensitive group in a review by Britto & Kronzucker (2002).

Aside from low growth rates, there are several indicators of ammonium toxicity in plants (Cramer & Lewis, 1993):

- chlorosis: yellowing of the leaves
- wilting
- reduced growth

- higher shoot-to-root ratios

Whereas the fundamental cause behind ammonium toxicity was previously believed to be the accumulation of $NH_3$ within the cell at high $NH_4^+$ concentrations and high cellular pH, it is now understood that this has little to do with it (Britto & Kronzucker, 2002). Instead, it is believed that at high concentrations ammonium diffuses through the $K^+$ channels in the plasmalemma. This leads to an accumulation of ammonium in the cytosol that suppresses the movement of other cations into the cell. It is believed that the low efficiency of ammonium expulsion from the cell needed to maintain cellular equilibrium ends up costing the plant too much energy to limit the ammonium concentration in the cytosol, creating the phenomenon of ammonium toxicity (AJ Miller & Cramer, 2004).

## 2.3 Hydroponic techniques

In order to properly plan a hydroponic experiment it is important to first know the best practice in hydroponics. This involves the conditions to be used and certain experimental techniques. It is also important to consider the pH and EC control strategies already employed in literature and industry in order to justify the control system proposed in this study.

### 2.3.1 Types of hydroponic systems

Many different hydroponic system exist with six of the most common shown in Figure 18.

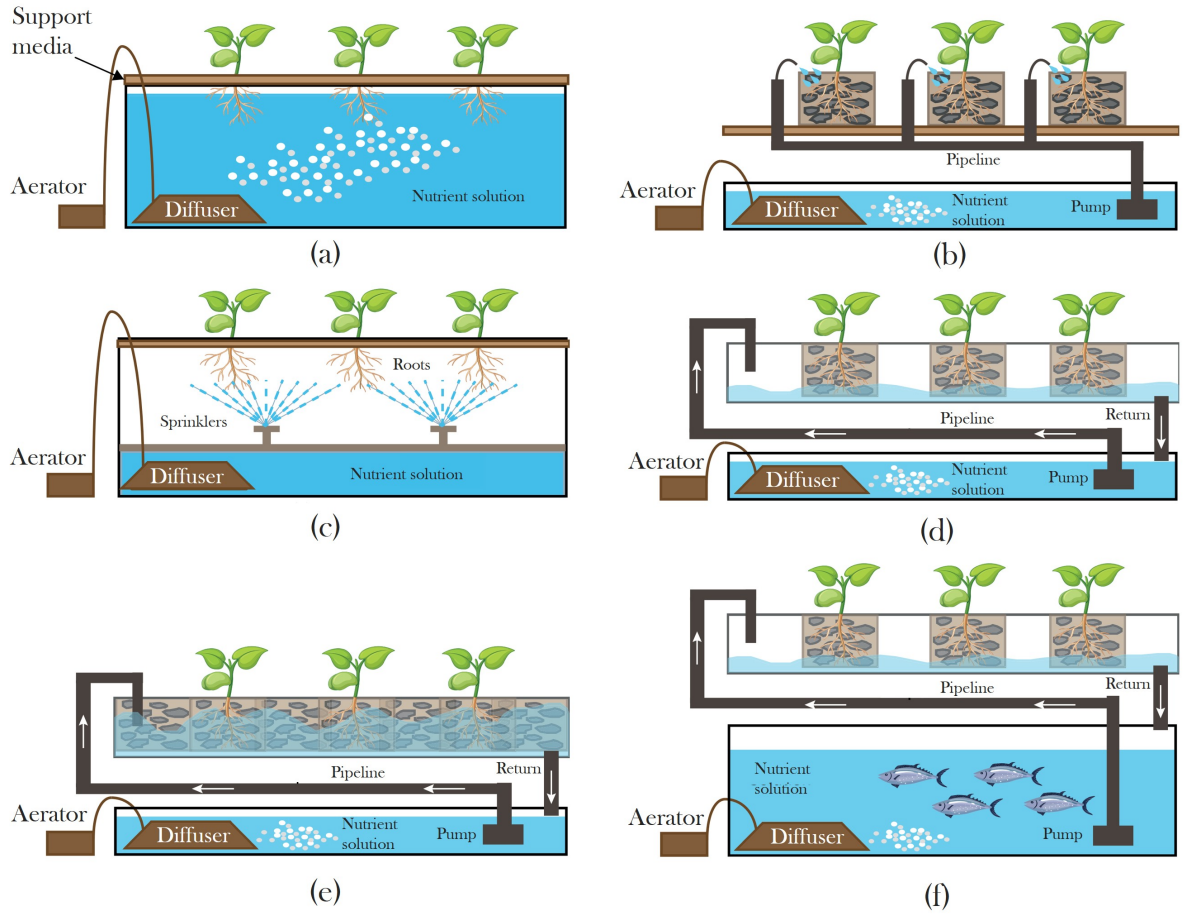


**Figure 18:** Different types of hydroponic systems. (a) is deep water culture, (b) is a drip system, (c) is aeroponics, (d) is the nutrient film technique (NFT), (e) is an ebb-and-flow system, and (f) is aquaponics (adapted from Velazquez-Gonzalez *et al* (2022)).

The system most commonly applied in practice is the NFT technique. However, this technique is not ideally suited to scientific study as the plants are not isolated. Instead most literature tends to use deep water culture. In this study ebb-and-flow shall be used. This has the advantage of isolating the plants while also providing excellent aeration to the root zone.

### 2.3.2 pH

It is generally accepted in the literature that the best pH range to operate in is pH 5–7 (Lu & Shimamura, 2018: 38). Anything below pH 4 risks poisoning the plant and anything above pH 8 leads to solubility problems. This range is ideal because it ensures the ions are available to the plant (through a combination of solubility and metabolic factors) at the concentrations applied in hydroponic nutrient solutions (Velazquez-Gonzalez *et al*, 2022).

The availability of the key nutrients are expressed by the Troug diagram in Figure 19.

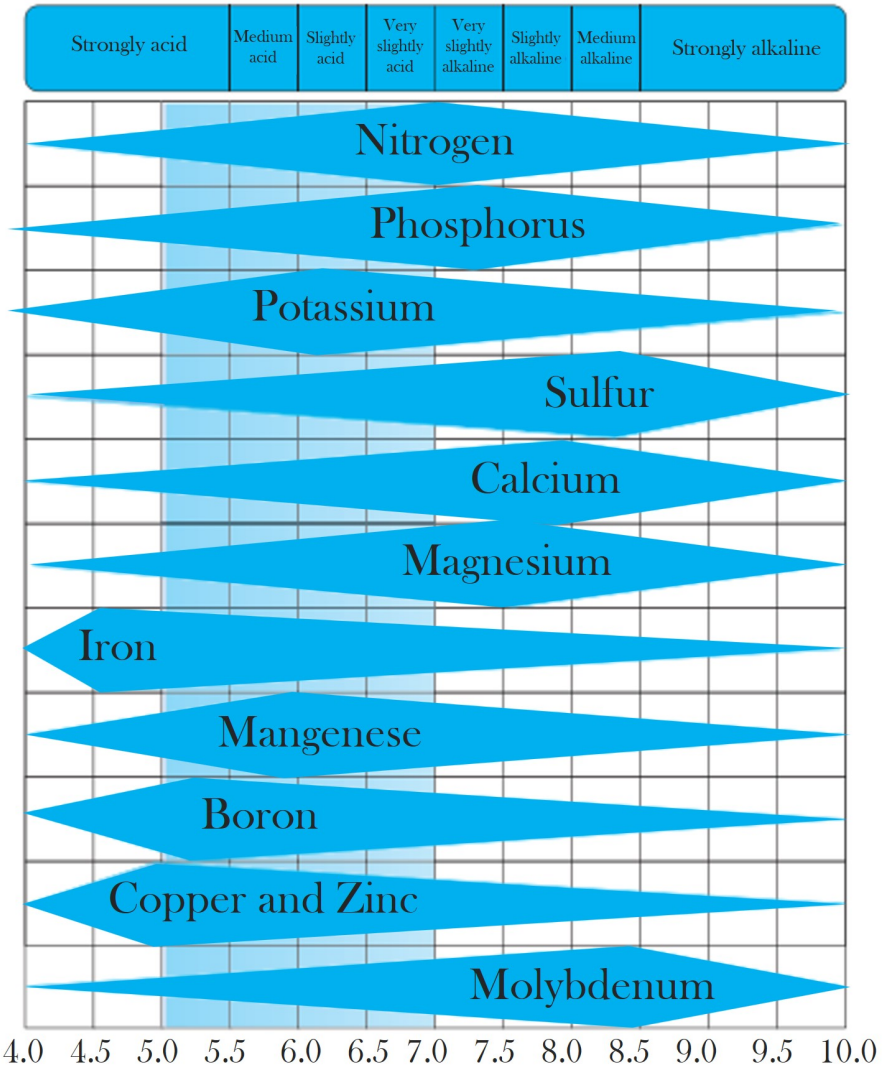


**Figure 19:** Availability of key nutrients across the pH range (adapted from Velazquez-Gonzalez *et al* (2022)).

Most studies dealing with kale tend to keep the pH just above 6. In the case of Assimakopoulou *et al* (2019) it was maintained in the range 6.0 to 6.5, while in the study conducted by Song, L Li, *et al* (2017) pH was adjusted daily to 6.2. Conversely, Wang *et al* (2022) allowed the pH to change freely (it generally stayed between 5 and 7) and went on to state that Chinese kale (a variant of *Brassica oleraceae*) was insensitive to pH in the range of 4.73–8.15. Moreover, Bugbee (2004) states that plants grow equally well between a pH of 4 and 7, with a slightly acidic pH being preferable. Thus, as long as the pH of the system is maintained around 6, then there should be no interference by pH with growth.

pH is often maintained via direct pH measurement followed by the addition of either an

acid or base (Ramazzotti *et al*, 2013; Velazquez-Gonzalez *et al*, 2022). A wide variety of acids and bases are applied to control pH, with nitric acid, citric acid, phosphoric acid, and hydrochloric acid being a few examples (van Rooyen & Nicol, 2021; van Rooyen & Nicol, 2022a; Kaewwiset & Yooyativong, 2017; Dunn & Singh, 2016). While very effective at controlling pH, the direct addition of acids like these have their problems. Firstly, hydrochloric acid, being a source of chloride, is obviously very bad in the long term as it will accelerate the build up of salinity within the growth medium, necessitating its replacement. Secondly, nutrient based acids (phosphoric and nitric acids) will interfere with the composition of the nutrient medium. To put this into perspective, for every mole of nitrate absorbed, half a mole of acid is required to restore the pH. If phosphoric acid were to supply all of the necessary protons in a nitrate heavy medium, one would be adding one mole of phosphate for every four moles of nitrate consumed; a phosphorus to nitrogen ratio around four times that recommended by Hoagland & Arnon (1938). A similar problem occurs with nitric acid, whereby in order to achieve the desired elemental balances and avoid adding too much nitrogen relative to the other nutrients, one is forced to adulterate the acid reservoir with an alternative proton carrier like hydrochloric acid (van Rooyen & Nicol, 2022a). All of these substances could also compromise the classification of the produce as organic as they are all synthetic (Williams & Nelson, 2016). Finally, carbon compounds like citric acid, would provide an attractive substrate for any bacteria in the medium. Considering the need for cleanliness within hydroponic setups, this is less than ideal (Fernandes, 2020; Velazquez-Gonzalez *et al*, 2022). Moreover, they tend not to be very effective at maintaining pH. Not only do bacteria feed off of them, plants also absorb them - often in an acidic reaction (Fernandes, 2020). Even if the system remained sterile, citric acid is more expensive than the inorganic alternatives, increasing the input costs of the system.

### 2.3.3 Electrical conductivity

Electrical conductivity (EC) is used as an indication of the salinity of a solution. It is proportional to the concentration of ions dissolved in solution and thus is often used to control the nutrient supply in hydroponics (A Miller, Adhikari & Nemali, 2020). However, when EC is too high it indicates a toxic build-up of ions, such that the solution becomes saline and must be replaced. Different plants can tolerate different EC ranges with kale preferring an EC range of 1.6 to 2.5 mS/cm (Patel, 2022). This is supported by Velazquez-Gonzalez *et al* (2022) who gives the EC ranges for broccoli and cabbage (both closely related to kale) as 2.8–3.5 mS/cm and 2.5–3 mS/cm, respectively. This suggests that kale could probably tolerate a higher EC than Patel (2022) suggests. In either case, the EC tolerance of kale is high and will likely not be a cause for concern in this study. However,

EC plays a pivotal role in inferring the nutrient concentration of the solution, and is used as such in this study. This shall be further expounded upon in Section 3.3.

### 2.3.4 Coupling pH and EC control

While both pH and EC need to be controlled (or at least maintained within certain limits), it is rare to find systems that couple the control of the two. As was stated in Section 2.3.2 and Section 2.3.3, pH and EC tend to be controlled independently with the addition of acid/base, and the addition of nutrients/dischanging of the nutrient solution, respectively. In a recent review of 19 hydroponic studies (Velazquez-Gonzalez *et al*, 2022), none were found to couple the pH and EC controllers in the way this study does. If they controlled pH and EC simultaneously, which they often are, they tended to rely on acid/base addition to control pH, and nutrient addition to control EC (Atmadja *et al*, 2017; Chang, Hong & Fu, 2018; Kaewwiset & Yooyativong, 2017; Saputra, Irawan & Nugraha, 2017; Ruengittinun, Phongsamsuan & Sureeratanakorn, 2017; Dunn & Singh, 2016). Several of the studies also relied on the buffering capacity of the nutrient solution alone, while others were more concerned with presenting monitoring systems without any control aspects.

The work within van Rooyen & Nicol (2021) and van Rooyen & Nicol (2022b) was the closest thing to coupled pH and nutrient concentration control that could be found. However, they still avoided directly measuring or controlling EC (or other indications of nutrient content), instead preferring to passively control it through the pH.

### 2.3.5 Means of quantifying nutrient uptake rate

As the study hinges on being able to link uptake rates with concentration, it is important that an accurate means of measuring uptake rate be developed. A common means of measuring nutrient uptake rate is the depletion method (McFarlane & Yanai, 2006). Essentially, this boils down to soaking of intact plant roots in water and measuring the change in water volume and nutrient concentration (Song, G Li, *et al*, 2016; McFarlane & Yanai, 2006). Variations of this method abound with several different pre-treatmemts having been tested by McFarlane & Yanai (2006) such as soaking the roots in solution to “condition” them but no change in uptake rates was seen in any of the pre-treatments relative to the control. This suggests that pre-treating the roots gives no additional benefit in terms of the accuracy of the measurement.

However, this study is not simply trying to assess the uptake preference of kale for ammonium and nitrate: it is undertaking to develop a control mechanism to leverage this

relationship. As such, mere depletion experiments are not sufficient. Instead the technique used by van Rooyen & Nicol (2021) where the dosing rate of nitrogen is used to calculate the uptake rate of the plants seems more appropriate. In this way, the uptake rate and preference of the plants can be inferred from online dosing data and daily ammonium and nitrate tests.

# 3 Experimental

There are two aspects to the experimental work. The first is a confirmatory experiment to prove that the relationship upon which the control system is based actually exists, while the second is to assess the efficacy of the proposed control system. These shall be referred to as the confirmatory experiment and the control system experiment, respectively.

All the plants used in this study were grown from kale seeds (*B. oleracea* var. *acephala* or Vate's Blue Curled Kale), purchased from Raw™ (1550 Printech Ave, Laserpark Ext 1, Honeydew 2040, Roodepoort, South Africa). All nutrient ions were provided by stock solutions that were made from analytical standard chemicals supplied by Merck (Darmstadt, Germany). Deionised water was used exclusively in all experiments for all applications that needed water.

## 3.1 Analytical instruments

A Cary 60 UV-Vis, G6860 A spectrophotometer (Agilent Technologies™, Santa Clara, California) was the only analytical instrument used in this study. It was used in conjunction with Merck/Supelco (Darmstadt, Germany) photometric tests to measure the solution concentration of ammonium, nitrate, and phosphate at wavelengths of 690 nm, 340 nm, and 690 nm, respectively.

## 3.2 Confirmatory experiment

The confirmatory runs took the form of a series of batch uptake experiments (similar to the studies by Song, G Li, *et al* (2016), Xiaochuang *et al* (2015), and Wang *et al* (2022) that explored the uptake rate of nitrogenous species by kale). The goal was to relate the uptake ratio of ammonium and nitrate to the concentration of ammonium and nitrate in the growth medium, and then compare this relationship to that derived from literature. Hence, the ratio of ammonium-to-nitrate in the nutrient solution was the independent variable while the dependent variable was the uptake ratio of ammonium-to-nitrate.

Each experimental run, of which there were eleven in total, consisted of between four and eight plants being placed in an aeroponic cloner (procured from hydrponics.co.za™) where the plant roots were suspended above sprayers in order to maintain a constant mist of nutrient solution around the roots. Each aeroponic cloner had a capacity of 10 L of nutrient solution. The plants were cultivated beneath Mars Hydro™ 400 W blue/red

LED lights (Mars II 400 LED Grow Light ©), producing 10 000 Lux at the canopy. Figure 20 depicts a schematic diagram of one aeroponic unit.

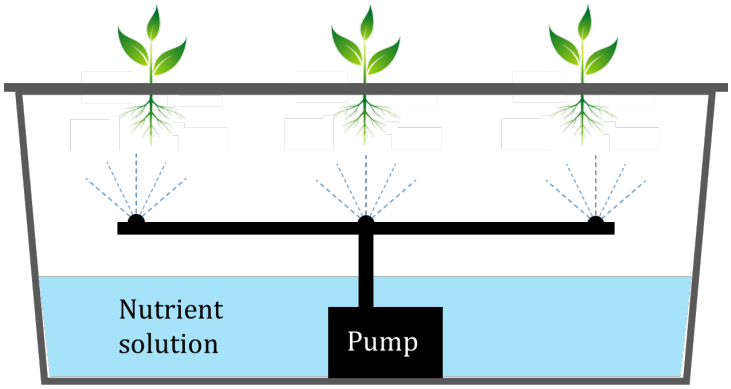


**Figure 20:** Aeroponic hydroponic system.

The ammonium-to-nitrate ratio of the nutrient solution that each confirmatory experimental run was initially charged with is summarised in Table 1. These nutrient solutions were composed so as to achieve similar ratios of elements as Hoagland solution while varying the ammonium-to-nitrate ratio (Hoagland & Arnon, 1938).

**Table 1:** The composition of the nitrogenous species charged into the system at the beginning of each run.

| Run | Initial concentration (mM) | |
|---|---|---|
| | Nitrate | Ammonium |
| 1 | 7.20 | 7.45 |
| 2 | 11.16 | 3.90 |
| 3 | 4.49 | 8.68 |
| 4 | 14.55 | 3.65 |
| 5 | 3.62 | 13.00 |
| 6 | 4.70 | 10.40 |
| 7 | 9.76 | 5.83 |
| 8 | 2.51 | 19.58 |
| 9 | 12.77 | 5.265 |
| 10 | 5.63 | 14.02 |
| 11 | 15.96 | 2.12 |

The ammonium and nitrate concentrations were measured over several days for each experimental run and the uptake rates of the two species calculated. These uptake rates were then related to the ammonium-to-nitrate ratio in the nutrient solution. This relationship was then compared with curves generated from published uptake kinetics of

other variants of *B. oleracea* to confirm that the relationship derived from manipulating the kinetic models existed in real life.

## 3.3 Control system experiment

The objective of this experiment was to trial the proposed control system. Three experimental runs were conducted in order to assess the efficacy of the system. The first experimental run, the sterile run, was a 21 day run in which the proposed control algorithm was used to maintain pH after the plants and apparatus had been sterilised with hydrogen peroxide. The sterile run served to show that the system worked according to the conditions upon which the underlying assumptions were based. The second was a non-sterile run. This was a 10 day run in which the proposed control algorithm was used to maintain pH where the plants and apparatus were unsterilised. The purpose of this run was to asses the robustness of the control system should bacteria – particularly nitrifying bacteria – colonise the system (Cytryn *et al*, 2012). In the third run, the system was fed with only nitrate. This was necessary to establish a baseline to which the proposed system could be compared, hence it shall be known as the baseline run.

All of the experimental runs for the control system experiment were carried out using an ebb and flow hydroponic apparatus consisting of four independent vessels. Each vessel had a volume of 1.64 L. An Arduino Mega 2560™ board was used to control all four vessels simultaneously. Haoshi™ pH probes ("pH meter Pro") were used to measure pH. These were calibrated using two point calibration where solutions of disodium hydrogen-phosphate and citric acid/sodium hydroxide/hydrogen chloride from Merck provided mV readings at 7 and 4, respectively. Gravity™ analogue electrical conductivity sensors V2 were used for the online measurement of EC. These, too, were calibrated using two point calibration with calibration standards included with the probes by the supplier. Kamoer © peristaltic pumps "Precision Peristaltic Pump + Intelligent Stepper Controller" were used for the dosing of nutrient solution – the exact composition of which depended upon the experimental run. DFrobot™ peristaltic pumps ("digital peristaltic pumps") were used for the addition of water to counteract the activity of transpiration. Xylem™ ("Flojet Diaphragm Electric Operated Positive Displacement Pumps, 3.8 L $min^{-1}$, 2.5 bar, 12 V DC") were used to circulate nutrient solution between the plant and the reservoir. Like the confirmatory experiment, the plants were cultivated beneath Mars Hydro™ 400 W blue/red LED lights (Mars II 400 LED Grow Light ©), producing 10 000 Lux at the canopy. A schematic diagram of one vessel in the the system is presented in Figure 21. The system consisted of four of these in parallel, each with a Mars Hydro™ 400 W blue/red LED light above it.

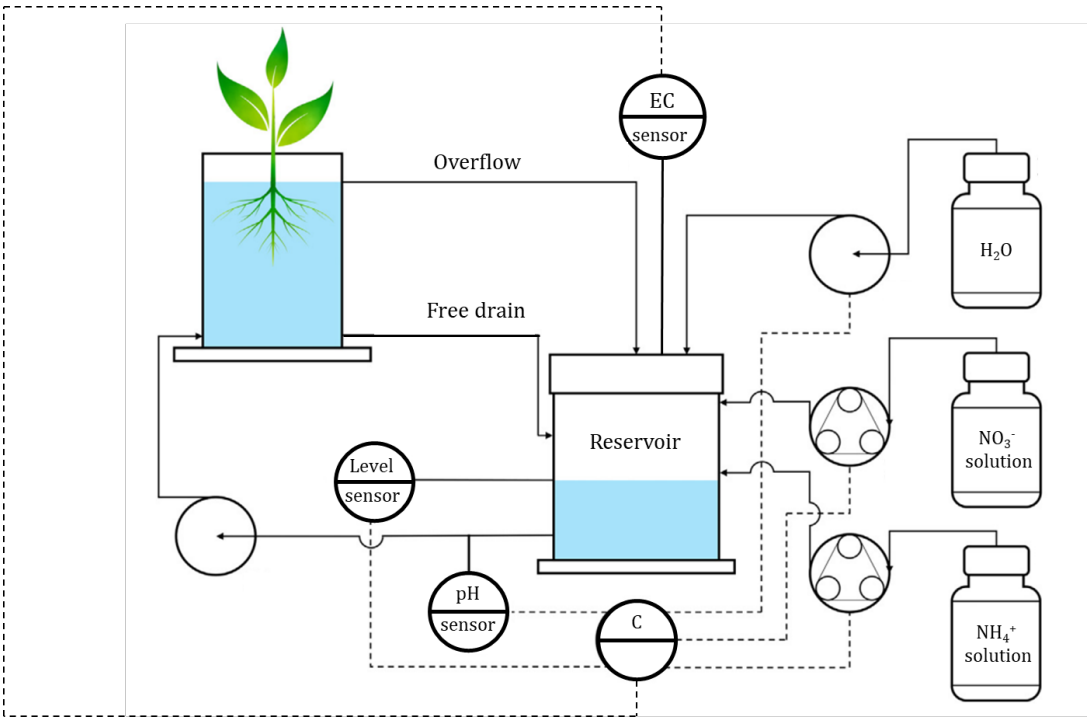


**Figure 21:** Schematic diagram of the ebb-and-flow hydroponic system.

Under normal operation, water is circulated between the reservoir and the plant continuously for 20 min. At this point the pump cuts out, allowing the system to drain freely back into the reservoir and measurements to be taken. This lasts roughly 10 min, after which the pumps resume circulating water between the reservoir to the plant. While the system drains, pH measurements are taken. Once the system has drained, the EC measurements are taken. The pH measurements have to be taken before the water level in the reservoir reaches the EC probes because the EC probes interfere significantly with the pH readings. Finally, the level of the system is measured with a float switch. If the level is too low, the float switch actuates an on/off controller that adds sufficient water to restore the water level, thereby keeping the volume of nutrient solution in the system constant.

Each run used plants that were cultivated from seed for roughly 28 days in the aeroponic cloners used for the confirmatory experiment. The plants were cultivated under a 24 h light cycle. After this time, plants of approximately the same weight (typically between 10 and 15 g) were transferred to the ebb and flow setup where the control system experiments were conducted. In order to eliminate the potential effect bacteria could have on the results of the sterile and baseline runs, the seedlings for these experimental runs were dosed with 0.3 mL of 90 % hydrogen peroxide every 3 to 5 days for the 28 days of their cultivation in the aeroponic cloners. Their roots were also soaked in 1 % hydrogen peroxide solution for 10 min before they were transferred to the ebb and flow setup.

Conversely, the plants for the non-sterile run were not exposed to hydrogen peroxide so that bacteria could be given the opportunity to establish themselves on the roots and hence allow for the assessment of the proposed control system in a comparatively less sterile environment.

As this is essentially a control system design, it is necessary to consider the variables in the context of control system design where one defines controlled variables, manipulated variables, and disturbance variables (Seborg *et al*, 2017: 3). There are two controlled variables: pH and EC. As such, there are two manipulated variables: N dosing rate and ammonium-to-nitrate ratio in the dosed N. Finally, there are two (important) disturbance variables: the nutrient uptake ratio of the plant and the nutrient uptake rate of the plant.

Figure 22 illustrates how the proposed control system functioned.

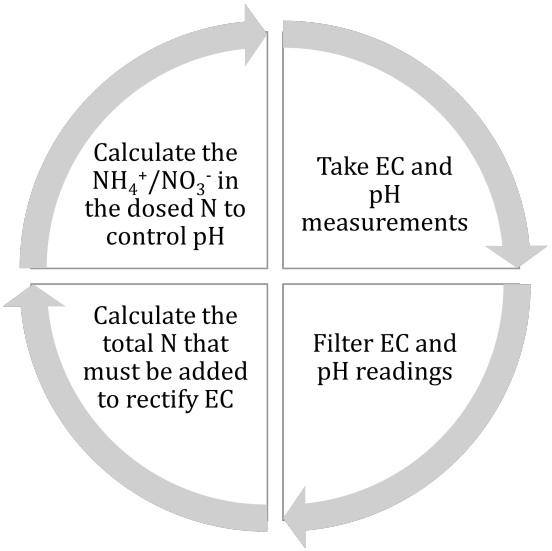


**Figure 22:** Schematic diagram illustrating the control action.

A PI control algorithm was used for EC control. Having determined the amount of total N to be added to the system in order to maintain EC, the controller calculated the fraction of this N that had to be dosed from the nitrate reservoir and the amount that had to be dosed from the ammonium reservoir. This fraction was calculated by a PID control algorithm.

In the sterile and non-sterile runs, two dosing reservoirs were necessary: one to provide ammonium and the other to provide nitrate. When the controller demanded ammonium be dosed into the system, the system drew from the ammonium rich reservoir. When the controller demanded nitrate be dosed into the system, the system drew on the nitrate rich reservoir. These two solutions were composed so as to achieve high concentrations of N and a balance of elements similar to that of Hoaglands solution while eliminating

precipitation. In order to achieve this, the interaction of the various ions had to be carefully considered to avoid the precipitation of any of the mineral salts. This was done by finding the solubilities of every possible ionic combination in Hoagland solution and then making up the dosing solutions in order to mitigate the possibility of precipitation. Table 2 summarises the solubilities of the various ionic combinations.

**Table 2:** The solubilities (mol/L) of the combinations of dominant anions and cations are shown below. These values were calculated from mg/100 mL solubility values in Green & Perry (2008).

| Nitrate reservoir | | | | | | | | |
|---|---|---|---|---|---|---|---|---|
| | | Cations | | | | | | |
| | | $Ca^{2+}$ | $Mg^{2+}$ | $K^+$ | $Na^+$ | $NH_4^+$ | $Fe^{3+}$ | $Cu^{2+}$ |
| Anions | $NO_3^-$ | 7.9 | 5.4 | 3.1 | 10.4 | 24.0 | 3.5 | 6.7 |
| | $SO_4^{2-}$ | 0.0 | 3.0 | 0.6 | 2.9 | 3.6 | 0.7 | 1.3 |
| | $PO_4^{3-}$ | 0.0 | 0.0 | | | | | |
| | $HPO_4^{2-}$ | 0.0 | 0.0 | | | 6.2 | | |
| | $H_2PO_4^-$ | 0.1 | 0.0 | 1.3 | 7.1 | | | |
| | $Cl^-$ | 6.7 | 5.7 | 4.6 | 6.1 | 7.0 | 4.3 | 5.7 |

| Ammonium reservoir | | | | | | | | |
|---|---|---|---|---|---|---|---|---|
| | | Cations | | | | | | |
| | | $Ca^{2+}$ | $Mg^{2+}$ | $K^+$ | $Na^+$ | $NH_4^+$ | $Fe^{3+}$ | $Cu^{2+}$ |
| Anions | $NO_3^-$ | 7.9 | 5.4 | 3.1 | 10.4 | 24.0 | 3.5 | 6.7 |
| | $SO_4^{2-}$ | 0.0 | 3.0 | 0.6 | 2.9 | 3.6 | 0.7 | 1.3 |
| | $PO_4^{3-}$ | 0.0 | 0.0 | | | | | |
| | $HPO_4^{2-}$ | 0.0 | 0.0 | | | 6.2 | | |
| | $H_2PO_4^-$ | 0.1 | 0.0 | 1.3 | 7.1 | | | |
| | $Cl^-$ | 6.7 | 5.7 | 4.6 | 6.1 | 7.0 | 4.3 | 5.7 |

It can be seen that the values in Table 2 are colour-coded. This colour coding has to do with the solubility of the ionic compound. White stands for soluble at the concentrations found in Hoagland solution, red stands for insoluble at the concentrations found in Hoagland solution, green stands for soluble at the concentrations found in Hoagland solution and that the ionic combination is present in the relevant dosing reservoir, yellow stands for ostensibly insoluble, but the concentration is so low that it can be accommodated in the dosing reservoir. There are two special cases. Firstly, $Fe^{3+}$, despite being soluble at the concentrations countenanced in the nitrate dosing reservoir, is excluded due to the tendency of iron to precipitate over time on exposure to light. Secondly, some of the red boxes have no numbers; this is because they were simply listed as "insoluble"

in Green & Perry (2008).

The composition of the dosing solutions are laid out in Table 3.

**Table 3:** Compositions of the dosing solutions. Both solutions were made up to a concentration of 150 mM N. Anions and cations refer to trace elements and were included in the nitrate dosing reservoir at 10 time the strength of Hoagland solution.

| Nitrate dosing reservoir | |
|---|---|
| Salt | Concentration (mM) |
| $KNO_3$ | 50 |
| $Ca(NO_3)_2$ | 50 |
| Cations | |
| Anions | |
| % of N as nitrate | 100 |
| % of N as ammonium | 0 |

| Ammonium dosing reservoir | |
|---|---|
| Salt | Concentration (mM) |
| $NH_4NO_3$ | 37.5 |
| $(NH_4)_2HPO_4$ | 4.5 |
| $NH_4H_2PO_4$ | 20.5 |
| $(NH_4)_2SO_4$ | 22.7 |
| % of N as nitrate | 25 |
| % of N as ammonium | 75 |

Undesirable ions like $Cl^-$ and $Na^+$ were able to be completely excluded through the use of phosphate buffering in the ammonium reservoir (A Miller *et al*, 2020). In an attempt to minimise the build-up of inert ions like $SO_4^{2-}$ (Maathuis, 2009), the ammonium dosing solution was adulterated with nitrate in the form of ammonium nitrate. The inclusion of 25 % nitrate reduced the need for phosphate and sulphate, while only slightly reducing the ability of the solution to alter the composition of the system (*i.e.* its potency). The composition is such that when fed in an ammonium-to-nitrate ratio of 33:67, the dosed ions will essentially mirror the elemental composition of Hoagland solution. This represents a significant benefit of this system over others that rely on a dedicated pH controller. Direct pH control ultimately requires the use of acids and bases like HCl and NaOH in order to achieve the appropriate nutrient ratios, and as such, leads to an accumulation of undesirable ions in the nutrient medium (van Rooyen & Nicol, 2021; van Rooyen, Brink & Nicol, 2021; A Miller *et al*, 2020).

Because $Mg^{2+}$ and $Fe^{3+}$ are only sparingly soluble at the concentrations involved, they

were added into the reservoir of the level control system at concentrations of 1 mM each. This meant that they were added proportionally to the rate of transpiration of the plants, which was found to be more-or-less proportional to nutrient demand.

The baseline run needed only one dosing reservoir where the necessary nutrients were dissolved in an acid solution such that the ratio of nitrate to protons was 1:0.6. This hypothetically allows for maintenance of both pH and [N] in the growth medium through the use of only pH measurement and one dosing reservoir (van Rooyen & Nicol, 2021). This composition of the dosing solution is the same as that used by van Rooyen & Nicol (2022a), with the addition of phosphate to balance the nutrient composition.

Similarly to the confirmatory experiments, the nutrient solutions charged into the system at the beginning of each control system experimental run were variants of Hoagland solution where the ratio of ammonium-to-nitrate was varied while attempting to keep the ratio of elements relatively constant. These compositions are detailed in Table 4.

**Table 4:** The composition of the nutrient solution charged into the system at the beginning of each run. Micronutrients were included but are not shown here.

| | Concentration (mM) | | |
|---|---|---|---|
| | Sterile run | Non-sterile run | Baseline run |
| $KH_2PO_4$ | 0.5 | 0.832 | 0.5 |
| $KNO_3$ | 1 | 3.324 | 2.5 |
| $Ca(NO_3)_2$ | 2 | 3.324 | 2.5 |
| $MgSO_4$ | 1 | 1.664 | 1 |
| $K_2SO_4$ | 3 | 0 | 0 |
| $(NH_4)_2SO_4$ | 1.25 | 1.664 | 0 |
| Nitrate fraction | 0.67 | 0.75 | 1.0 |

Daily measurements of the concentration of ammonium, nitrate, and phosphate, as well as plant mass, were made for each experimental run. The ammonium and nitrate measurements were to see if the system was actually operating at the anticipated ammonium-to-nitrate ratio suggested by modelling, while the phosphate measurement was to gauge the extent of phosphate accumulation/depletion, serving as a bellwether for salt accumulation.

At the end of each experimental run the plants were dried in an oven at 60 °C until they achieved constant mass. The dry leaf matter was then milled in a Retsch ball mill with the resultant finely ground leaf material analysed for nitrate, ammonium, total nitrogen, chlorophyll, and ash fraction.

Nitrate content was obtained by the method outlined by Zhao & Wang (2017) with the exception that the plant leaves were dried and crushed instead of frozen. Ammonium content was analysed for using an analogous method to that outlined by Zhao & Wang (2017) where the leaves were similarly dried and Merck-Spectroquant tests were used to measure ammonium content instead of the salicyclic acid method. Both of these tests were conducted in triplicate. Elemental analysis was conducted by the Department of Chemical Engineering of the University of Pretoria on the dried leaves of all of the plants in the sterile and baselines runs, and Plant 2 and Plant 3 of the non-sterile run. The protein content of the leaves was calculated by subtracting the amount of nitrogen in ammonium/nitrate from the total nitrogen. This new value was then multiplied by 5.77 to convert from the mass of nitrogen to the mass of protein. 5.77 is the mass of protein per mass of nitrogen contained in protein and is based on the general formula $C_nH_{1.58n}N_{0.28n}O_{0.30n}S_{0.01n}$ (Torabizadeh, 2011).

The ash content of the leaves was found by weighing known amounts of the dried, crushed plant leaves into crucibles and placing these in a furnace at 850 °C for 8 hours. This was done in triplicate.

The chlorophyll content of the leaves was assessed by soaking ±0.02 g of dried and ground leaf matter in 8 mL of 80 % acetone – 20 % water (volume basis) for 24 hours. The supernatant was then centrifuged and the absorbance of the supernatant at 663 nm and 645 nm was measured and used in conjunction with the equations developed by Arnon (1949). The results were compared against those derived from the newer model detailed in Porra (2002). Little difference between the two was found, so it was decided that the results from the more widely used Arnon (1949) model would be the ones considered.

The experimental results were analysed using ANOVA (Diez, C¸etinkaya-Rundel & Barr, 2019: 285) and t-testing (Diez *et al*, 2019: 267) where the Welch–Satterthwaite equation was used to calculate the degrees of freedom in the t-tests (NIST, 2023).

The success of the proposed control system was based on its performance as compared to the more traditional approach embodied by the baseline run. To be considered a success, it must at least achieve similar crop yields, with any nutritional benefits on top of this being an added bonus.

# 4 Results and discussion

The results and discussion are considered under three subsections, under which the results are presented and discussed *in-situ*. The first subsection chronicles the results of the confirmatory experiment. The second subsection details the creation of the computer model and the tuning of the controller. The third subsection presents and discusses the results of the control system experiments, where the control system is trialled in real life.

## 4.1 Quantification and confirmation of the relationship between uptake ratio and concentration ratio

Underpinning this whole study are two assumptions. The first is that in the presence of a growing medium of Hoagland solution, every mole of nitrate absorbed by a plant is accompanied by 0.5 mol of protons also being absorbed (thereby releasing 0.5 mol of $OH^-$ into the growing medium) and that for every mole of ammonium absorbed by a plant, 1 mol of protons are released into the growing medium. These values are based on a study by van Rooyen & Nicol (2022b). The second assumption is that *B. oleracea* selectively absorbs ammonium and nitrate at rates that are dependent upon the the concentration of the two ions in the growing solution. If these two assumptions are correct, then it should be possible to operate the system at an ammonium-to-nitrate ratio in such a way that pH remains constant because the number of protons withdrawn and released from the solution is balanced. Hence, the pH homeostasis point will be the ammonium-to-nitrate ratio where the nitrate uptake rate is double that of ammonium.

While the first assumption is backed up by literature, the second was affirmed here by manipulating uptake rates from literature so as to relate uptake rate ratio with concentration ratio and then comparing this mathematical relationship to experimental results. The uptake kinetics proposed by Song, G Li, *et al* (2016) and detailed in Section 2.1.7 are the ones used in modelling. The exact parameters are detailed in Table 5.

**Table 5:** Kinetic parameters for the uptake of ammonium and nitrate. $NO_3^- + NH_4^+$ refers to the uptake rate of nitrate when some $NH_4^+$ was also present in the solution. $g_{FW}^{-1}$ refers to the fresh mass of roots.

| | $K_m$ (mmol/L) | $V_{max}$ ($\mu$mol.$g_{FW}^{-1}$.$h^{-1}$) |
|---|---|---|
| $NH_4^+$ | 3.598 | 21.2 |
| $NO_3^-$ | 3.322 | 29.5 |
| $NO_3^- + NH_4^+$ | 3.329 | 26.1 |

Using these kinetic parameters, estimates of the rate of ammonium and nitrate uptake at different concentrations of ammonium and nitrate were made. The relationships defined in Table 5 between uptake rate and concentration are plotted in Figure 23a.

If one keeps total nitrogen concentration ([N]) constant while varying ammonium-to-nitrate ratio, it is possible to generate a plot comparing how the nitrate uptake ratio varies with the nitrate concentration ratio. This is presented in Figure 23b.

Assuming the proton ratios identified by van Rooyen & Nicol (2022b) remain relatively constant with concentration, it should be possible to manipulate the pH of the system by adding ammonium/nitrate in such a way so as to move along the curve in Figure 23b. As ammonium is added, the nitrate fraction decreases, encouraging the plant to absorb more ammonium, thereby lowering pH as more protons are released. As nitrate is added, the nitrate fraction increases, encouraging the plant to absorb more nitrate, thereby increasing pH as more protons are removed from solution. Thus, it is possible to control pH just by strategically adding nutrient solution that is either heavy in ammonium or heavy in nitrate.

The confirmatory experiments took the form of several batch experiments. Although the concentrations were not kept constant in the confirmatory experiments (unlike in Figure 23b), the general shape and pH homeostasis point are similar to that derived from literature. The two plots derived from literature and the data from the confirmatory experiments are presented in Figure 23.

It is clear from Figure 23c that the uptake ratio shows the same dependency on concentration ratio as theory suggests. It can also be seen that the pH homeostasis point is roughly in the range 67 % to 79 %. The higher the total nitrogen concentration, the higher the pH homeostasis point.

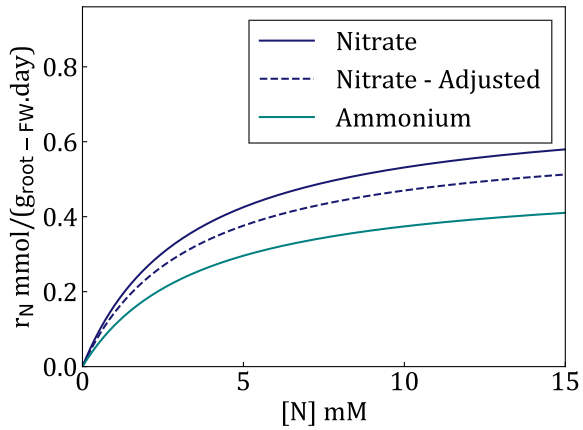


**(a)** Uptake rate of nitrogenous species as concentration changes. "Nitrate - adjusted" refers to the uptake rate of nitrate in the presence of ammonium.

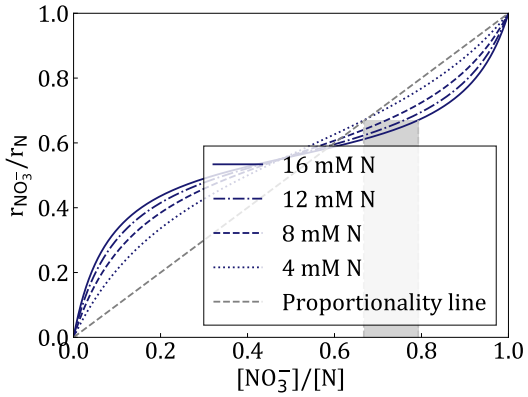


**(b)** Uptake ratio versus concentration ratio of nitrate. Each curve refers to a constant total nitrogen concentration. The grey area refers to the range of pH homeostasis points.

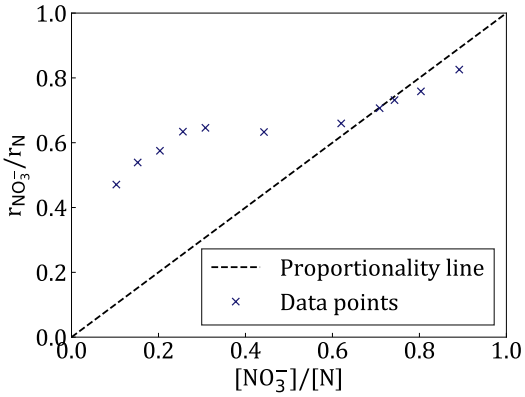


**(c)** Results of batch experiments testing the relationship between concentration ratio and uptake ratio.

**Figure 23:** Uptake kinetics of ammonium and nitrate from literature and experimentation.

## 4.2 Computer modelling and controller design

Having proven that the literature equations adequately describe the behaviour of the system, a computer model of *B. oleracea* var. *acephala* was constructed so that different control strategies could be trialled virtually before real life experiments were conducted. Python was used as the coding language. The model sought to simulate the pH, EC, and ammonium, nitrate and phosphate concentrations of the growing medium in the face of disturbances introduced by the plant and the resultant control action. Six key assumptions were made to simplify the design of the model:

1. The uptake rates of $NH_4^+$ and $NO_3^-$ follow the Michaelis-Menten kinetics kinetics identified in Table 5 (specifically the first and third rows).

2. The growth rate of the plant followed the same time dependency of an unpublished experiment. It was assumed to be independent of growth conditions like pH, EC, and nutrient concentrations.
3. EC was linearly correlated to $[NH_4^+]$ and $[NO_3^-]$.
4. The plant is the only living thing in the system capable of interacting with the growth medium (*i.e* the activity of nitrifying bacteria are neglected).
5. 1 mol of protons are released for every mole of $NH_4^+$ absorbed by the plant.
6. 0.5 mol of protons are absorbed for every mole of $NO_3^-$ absorbed by the plant.

The computer model made use of the Euler method for solving differential equations (Labuschagne *et al*, 2018: 67). In order to simulate the control system, control action was only undertaken every 30 minutes (each time step was 1.38 s, so there would have been 1300 time steps between measurements, approximating a discreet control system working on a continuous system) (Seborg *et al*, 2017: 133). The differential equations governing nitrate/ammonium uptake were the Michaelis-Menten kinetics in the first and third rows of Table 5. The uptake rate of phosphate was assumed to equal one fifteenth that of the total nitrogen uptake rate. This was based on the ratio of nutrients in Hoagland solution. pH and phosphate dissociation were calculated using the proton flux due to ammonium/nitrate uptake and its influence on the dissociation of water and phosphate.

Gaussian noise was introduced to reflect the natural variation in measurement about the "true" value (S Miller & Childers, 2021; element14, 2021). Double exponential filters were applied to both the EC and pH controllers to moderate the effect of this noise on readings (Seborg *et al*, 2017: 304).

The exact details of the equations applied are shown in Appendix A.

Numerous control architectures for the EC and pH were trialled. These included simple on/off control, proportional control, PI control, and PID control. It was found that EC could be adequately controlled by PI control while pH required PID control with a very prominent differential contribution. The reason for this was the slow dynamics of the system. Instead of controlling pH directly, the system manipulates the ammonium-to-nitrate ratio of the growing medium so as to encourage the the plant to push the pH back to the set point by absorbing ammonium and nitrate in a specific ratio. As such, the rate at which pH can be changed is dependent upon the rate at which the plant takes up nutrients. Proportional and PI control often overshot the pH set point, leading to severe pH oscillations. Differential control was necessary to iron out these pH swings

by reversing the direction of the controller depending on the rate of change of the pH, thereby avoiding drastic oscillations. The position forms of the PID and PI digital control algorithms were used (Seborg *et al*, 2017: 133). These are expressed by Equation 3 and Equation 4, respectively

$$p_k = \overline{p} + K_{c,pH}\left[e_k + \frac{\Delta t}{\tau_{I,pH}}\sum_{j=1}^{k} e_j + \frac{\tau_D}{\Delta t}(e_k - e_{k-1})\right] \tag{3}$$

$$p_k = \overline{p} + K_{c,EC}\left[e_k + \frac{\Delta t}{\tau_{I,EC}}\sum_{j=1}^{k} e_j\right] \tag{4}$$

$p$ is the controller output, $\overline{p}$ is the initial controller output, $e$ is the error between the measurement and the set point, $\Delta t$ is the time between control actions, and $K_c$, $\tau_I$, and $\tau_D$ are control parameters. The control parameters were decided via trial-and-error using the computer model to see which combination gave the best pH control.

The control parameters that were found to give the best control are presented in Table 6.

**Table 6:** Control parameters found to give good pH control based on the model and applied in the experimental work.

| | | |
|---|---|---|
| $K_{c,pH}$ | 0.75 | |
| $K_{c,EC}$ | 0.002 | mol N.cm/($\mu$S) |
| $\tau_{I,pH}$ | 0.7 | days |
| $\tau_{I,EC}$ | 1 | days |
| $\tau_D$ | 6 | days |

Figure 24 shows a typical pH curve produced by the computer model. This should give an idea of the quality of pH control possible.

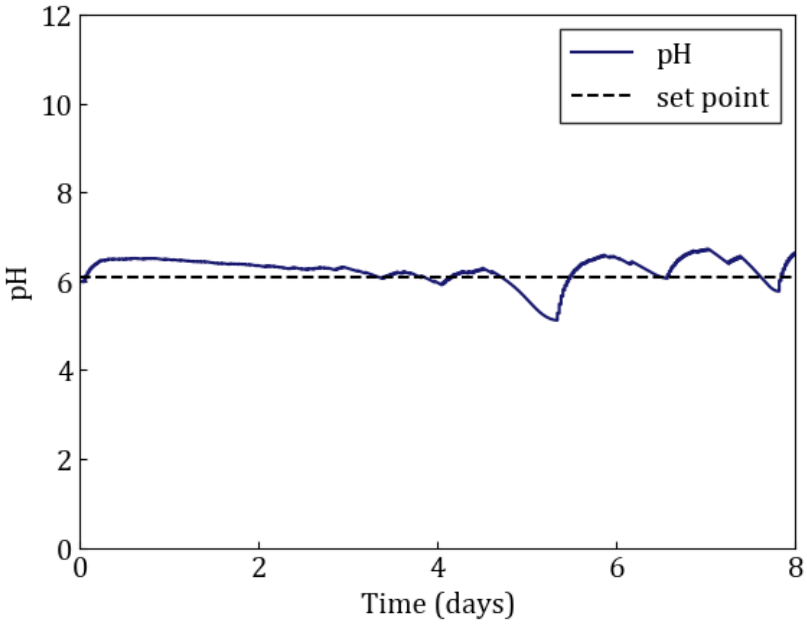


**Figure 24:** pH profile generated by the computer model

It can be seen that pH changes only slowly in the beginning, indicating good pH control. However, as the simulation runs on, the swings in pH become larger. This is an artefact of the nature of this sort of system where the subject under control grows exponentially. As the plant grows, its capacity to absorb nutrients expands as well, resulting in more nutrients being withdrawn from the medium. As more nutrients are absorbed, more protons are released/absorbed from the the medium, resulting in bigger pH changes. Thus, as the plant gets bigger, it can be thought of as "outgrowing" the tuned parameters. While this was not a problem in this short simulation, this tendency must be carefully considered in real world experiments.

## 4.3 Control system experimental results

The results of the control system experiment shall be considered under several different headings, each of which discuss a certain aspect of the control system. The complete complement of statistical analyses are presented in Appendix B.

### 4.3.1 Successful simultaneous control of pH and EC using ammonium and nitrate

The results of the sterile and non-sterile runs are shown in Figure 25.

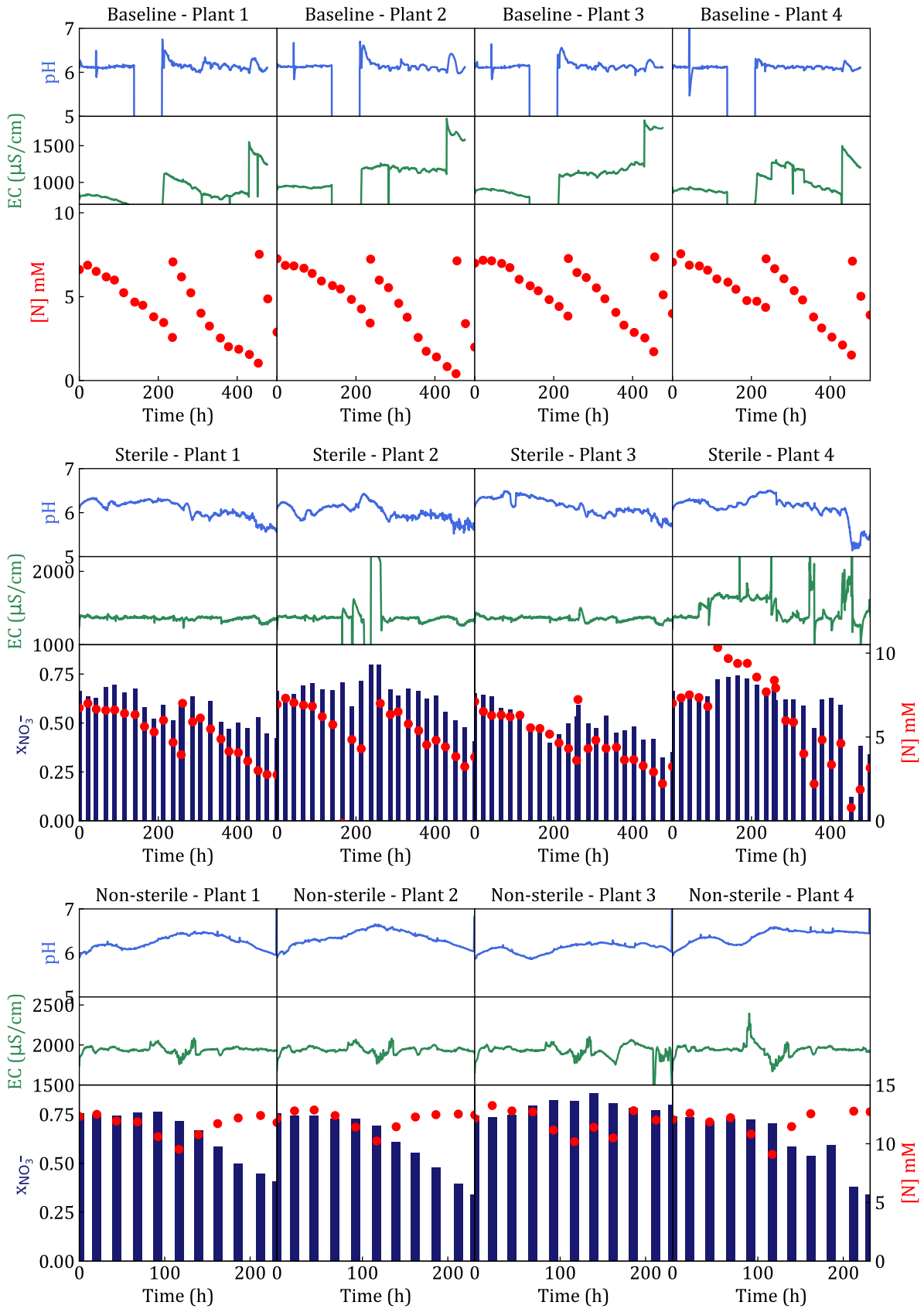


**Figure 25:** Online measurements of EC and pH compared to concentration and dosing data.

It is clear that in both the sterile and non-sterile runs that the system successfully controlled pH within the bounds of 5 and 7. pH control was actually much tighter than the required range, never deviating more than 0.5 from the set point of 6.1 except in cases of component failures. Both the sterile and non-sterile runs witnessed gradual pH oscillations around the set point with the pH getting "stuck" either above or below the set point before corrective action caused it swap sides. Similarly to the results of the computer model, these sustained periods of operation just above or below the set point appear to be an artefact of the heavy differential action of the controller that tended to suppress the movement of the controlled variable away from its current value. The gradual downward trend in pH seen in the sterile and non-sterile runs is also a result of this.

While pH was relatively smooth, the EC readings for the sterile run proved to be much bumpier. This can be largely explained as being the result of a few minor component failures. Firstly, the level control for Plant 2 failed during day 10. This meant the probe was not submerged, leading the system to dose excessively and causing the EC spikes visible at this time. In addition to this, the EC probe for Plant 4 was repeatedly poisoned, causing it to give abnormally large readings. When this was detected the probe was washed in deionised water, after which the readings normalised. These abnormal readings never lasted more than a day and hence are not believed to have significantly affected the results for Plant 4. The solution was replaced once on day 11 for all the plants in both the sterile and baseline runs with a second solution replacement on day 19 for the baseline run, hence why the big jumps in [N] are observed at these times.

Conversely, these breakdowns serve to further illustrate the effectiveness of the control system. It can be seen that the pH of Plant 4 in the sterile run collapsed at about 400 hours due to the momentary suspension of dosing owing to the poisoning of the EC probe surface. The fact that pH went haywire when control action was disabled shows that the control system was what was keeping pH stable.

While the non-sterile run suffered no major disruptions, the baseline run suffered two periods of suspended operation due to power cuts caused by blackouts in the local grid. While neither of these lasted much more than twelve hours, their presence in the data (visible in the big gaps in EC and pH in Figure 25) is exaggerated because they deleted several hours worth of data before the blackout. More importantly, these periods of suspended operation appeared to have no material effect on the results, judging by the trends in growth characteristics presented in Figure 26 under Section 4.3.2.

Although [N] declines during the course of the sterile run, it never drops to the point where it would stymie growth. The fact that it drops in the first place while EC remains

constant suggests that inert ions are building up and replacing the N containing species. This is partly due to metal ions, but the most prominent ion that builds up is likely sulphate. This is because sulphate is supplied in excess of the ratio recommended by Hoagland & Arnon (1938). Considering that sulphate is non-toxic (Maathuis, 2009), this is a fair trade-off as it allows for the omission of more harmful ions like chloride that would have been used in its place.

It is also likely a result of operating at a lower nutrient concentration. The non-sterile run witnessed very little deterioration in the relationship between EC and [N] while operating at a higher N concentration compared to the sterile run. Higher N concentrations will have the effect that nutrient uptake rates will be higher, particularly in the case of ions that are predominantly taken up passively, like $Ca^{2+}$. This, in turn, reduces the accumulation of inert ions by encouraging their uptake by the plant. Moreover, it would seem that the controller found it easier to control EC at higher EC and [N] values. This can be seen in the slight downward trend in EC observed in the sterile run. Although small, this mild downward drift in EC corresponds to a very significant decrease for [N]. This is because [N] appears to be very sensitive to EC, highlighted by the small dip in EC at 125 hrs in the non-sterile run causing a major drop in [N] before recovering. This problem can be easily addressed by using a more aggressive EC control algorithm. Despite this, it is clear that the control system continued to supply the plants with a sufficient supply of nutrients so as to avoid inhibiting growth.

### 4.3.2 Absence of ammonium toxicity

It would seem that ammonium toxicity was successfully avoided by the control system. The visual signs of ammonium toxicity (as detailed under Section 2.2.4) were absent in the plants involved in the sterile and non-sterile runs. Figure 26 shows the growth characteristics of the three treatments.

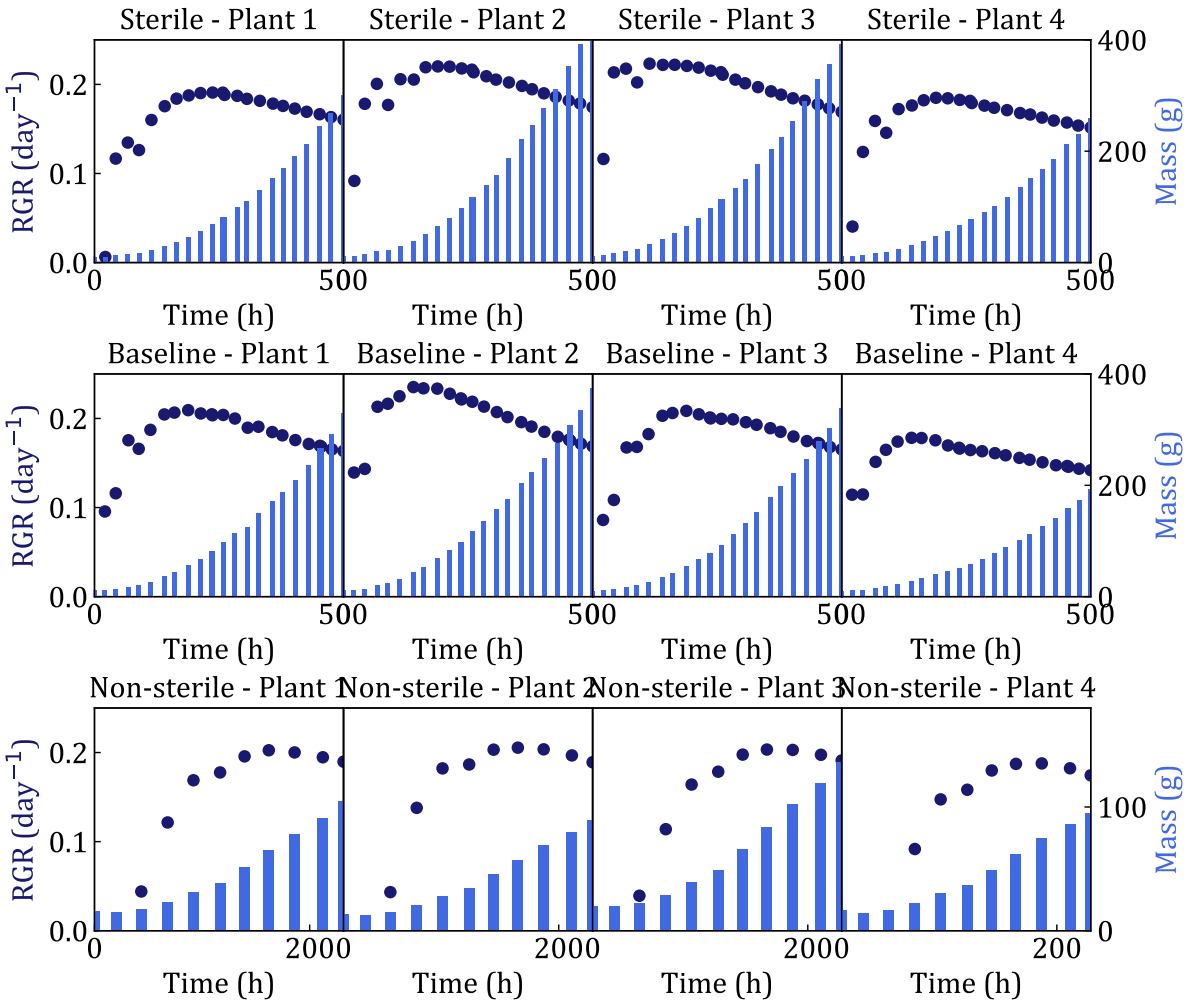


**Figure 26:** The daily measures of plant mass and the subsequent RGR. The largest RGR was used as the maximum, or "peak", RGR.

As was discussed under Section 2.2.3, ammonium fractions beyond 50 % of total nitrogen in the nutrient solution have generally been found to inhibit growth in *B. oleracea* (the most systematic sign of ammonium toxicity) with the best growth rates in literature being at around 25 % (Wang *et al*, 2022; Assimakopoulou *et al*, 2019). In principle, the system should have operated at about 70 % nitrate (corresponding to 30 % ammonium) as a fraction of total nitrogen, putting it safely out of the range where ammonium toxicity manifests. In reality, the system tended to operate more in the region of 50 % nitrate, skirting the danger zone. Despite this, no symptoms of ammonium toxicity were observed. Chlorosis was absent in virtually all of the plants (and where it was present it could be linked to nutrient deficiencies when the plant was in the nursery) and any wilting was transient. More importantly, the growth rates of all the plants involved were very healthy. Because of the variety of starting sizes of the plants and the vast difference in length between the runs, growth was compared by calculating daily relative growth rates (RGRs) for each plant, with the maximum representing the "true" value of the RGR.

These RGR curves are shown in Figure 26.

RGR can be seen to rise rapidly and then steadily decreases. The rapid rise is likely the result of the plant recovering from the shock of transplantation as well as a positive response to being moved to a location more conducive to growth. Conversely, the decline is likely due to increasing plant size. As the plants get bigger, they would have to divert a greater share of energy to maintenance as opposed to growth. This would be exacerbated by the leaves exploiting the maximum available light once they achieve full coverage of the available area (*i.e.* leaves growing on top of each other will not absorb additional light). It is apparent from Figure 26 and Figure 27 that there is no significant difference between growth rates across the the different treatments.

However, RGR is only half the story when considering the yield of plants. The most commercially valuable part of the plant is the leaves, which represent the edible part of the plant. Because of this it is important to know the effect of the different treatments on the leaf fraction of the plant. The relevant growth metrics are presented in Figure 27.

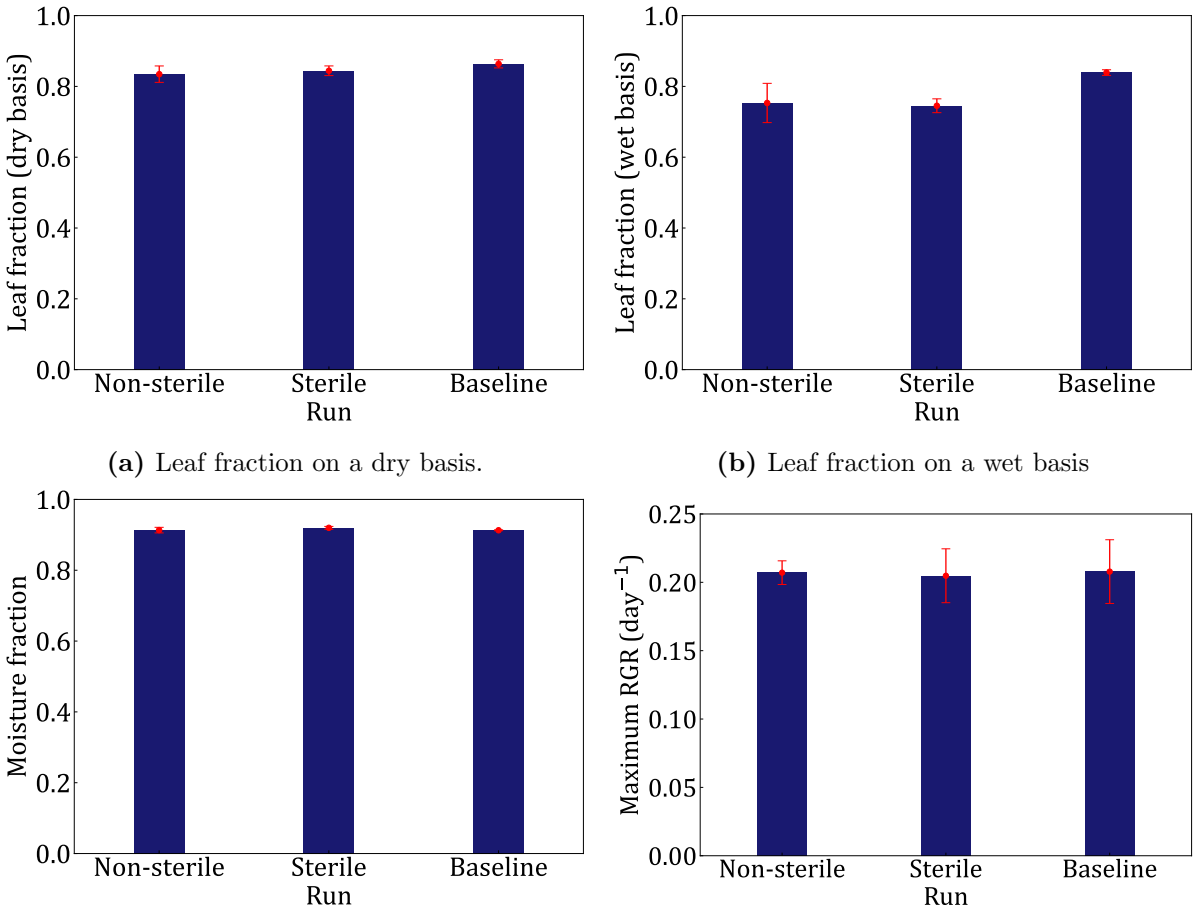


**(a)** Leaf fraction on a dry basis.

**(b)** Leaf fraction on a wet basis

**(c)** Moisture fractions of the plants.

**(d)** Maximum RGRs of the plants.

**Figure 27:** Growth metrics of the three experiments. Error bars represent standard deviation where n = 4.

At first glance, the mass of leaves as a fraction of the total plant mass is appreciably higher in the nitrate treatment than in the ammonium treatments. However, when considering the dry mass fraction, the gap narrows considerably. Coupled with the fact that the growth rates and moisture fractions are essentially the same across all of the treatments, the biomass yield of the three treatments is very close. This conclusion is further supported by ANOVA conducted on the maximum RGR data, leaf fraction (dry basis), and moisture fraction that found there to be no significant difference between the different runs on a 5 % confidence interval. Interestingly, while ANOVA found no significant difference in moisture fraction, t-testing found a statistically significant difference to exist between the sterile and baseline run. However, this amounted to a fraction of a percent (92.0 % versus 91.3 %) and thus hardly serves as an indictment on the performance of the sterile run.

This indicates conclusively that ammonium toxicity has not manifested as the growth rates are the same and the yields of leaf matter are similar.

### 4.3.3 Significant contribution of bacteria to nitrogen uptake characteristics

Figure 28 shows the dosing of ammonium and nitrate in twelve-hour time intervals and how the cumulative amount dosed varied with time.

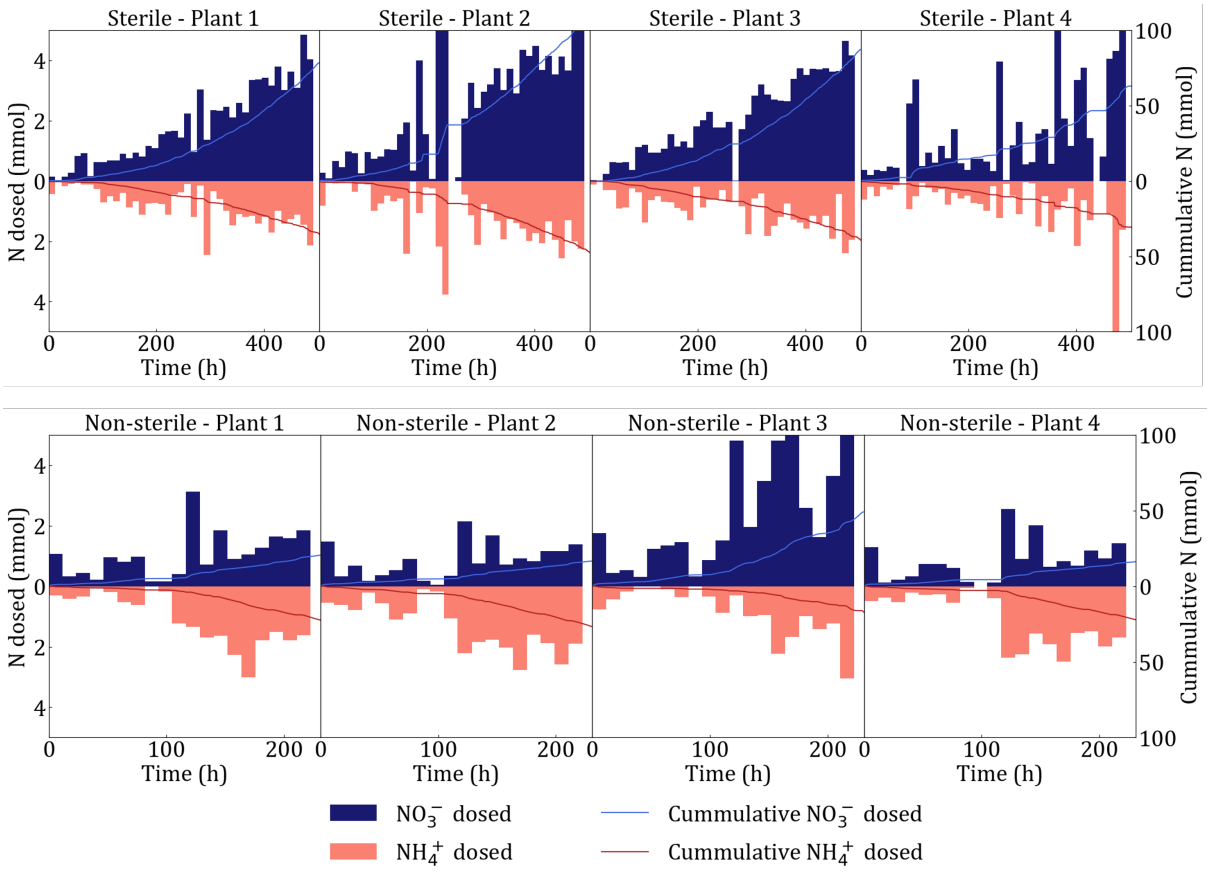


**Figure 28:** Dosing data for the experiments.

Figure 29 compares the cumulative fractions of nitrate dosed and absorbed in the non-sterile and sterile runs.

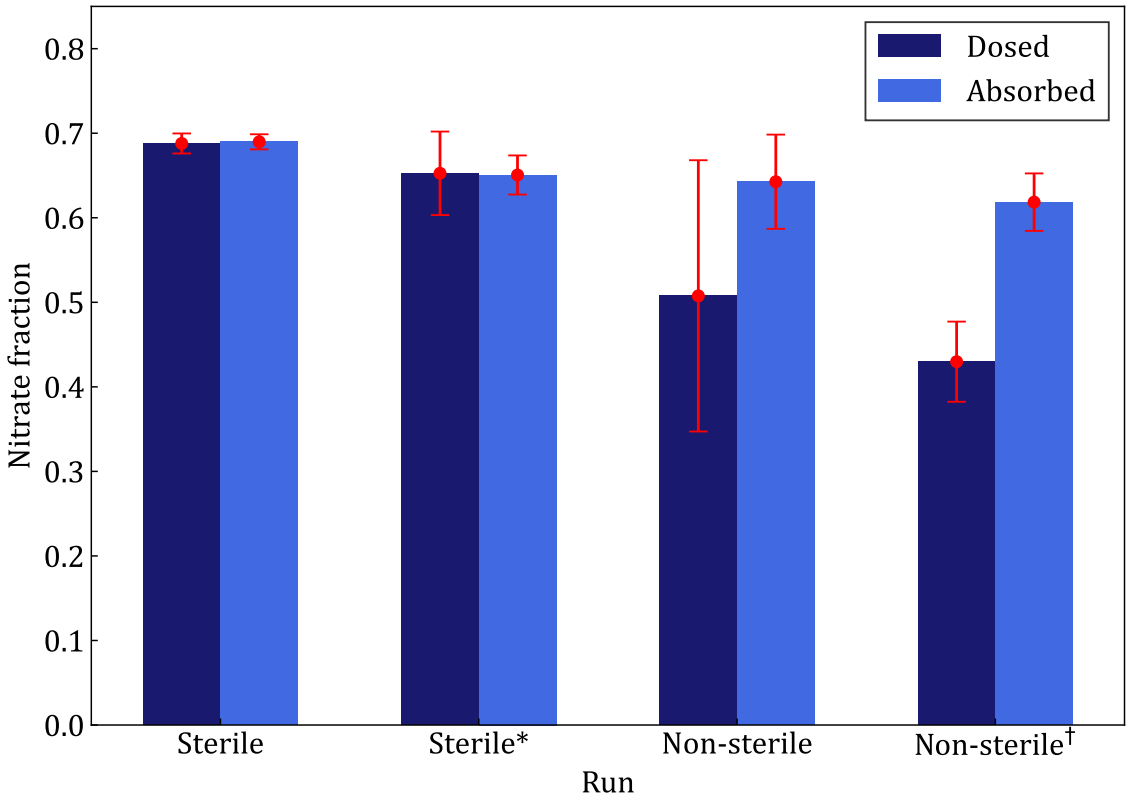


**Figure 29:** Nitrate as a fraction of the total amount of nitrogen dosed to the system and absorbed by the plant. Error bars represent a standard deviation where n = 4. Sterile* refers to the first 210 hours of the sterile run (this is equivalent to the length of the non-sterile run). Non-sterile† refers to the data for Plants 1, 2, and 4 (hence n = 3 for this data set).

Although the fraction of nitrate to total nitrogen concentration in solution deviated quite significantly from the expected value of 70 % needed to maintain pH, the ratio of nitrate to total nitrogen supplied and consumed cumulatively during the sterile run was close to the 67 % calculated from literature (68.8 % and 69.0 %, respectively). This shows that the underlying assumption of 0.5 mol of protons being absorbed for every mole of nitrate absorbed (thereby releasing 0.5 mol of $OH^-$ into the growing medium) and 1 mol of protons being released for every mole of ammonium absorbed, is sound.

There are two big differences between the sterile and non-sterile runs that are apparent from Figure 29. The first is the higher variability of the non-sterile run as compared to the sterile run. Part of this can be attributed to the shorter length of the non-sterile run (as evidenced by how the error bars of the "Sterile*" data set are wider than those of the "Sterile" data set). However, even after this adjustment is taken into account, the error bars of "Non-sterile" are still clearly much larger. Although there are numerous reasons for why the two runs should differ, such as differing starting [N] and run-time, the most plausible explanation would seem to be the infiltration of the non-sterile run by bacteria

(as was the intention). The presence of free ammonium and the absence of high carbon concentrations in the nutrient medium should prove especially attractive to nitrifying bacteria; a family of bacteria that respire by oxidising ammonium-to-nitrate (Madigan *et al*, 2022: 530). It is known that nitrifying bacteria rapidly colonise hydroponic systems (Cytryn *et al*, 2012), further supporting the hypothesis that nitrifying bacteria have taken up residence in the system. Moreover, nitrifying bacteria are known to live in discreet colonies (Silber & Bar-Tal, 2008: 300) – they do not propagate homogeneously throughout a medium – explaining the unpredictable behaviour among the four plants as a result of each hosting colonies of differing size (and likely differing consortia) on their roots.

Further proof that bacteria had established themselves in the rhizosphere was apparent from the results of the ash analysis. The ash from the non-sterile run was a vivid blue colour, while that of the sterile and baseline runs was much closer to white. Bacteria are known to enhance the ability of plants to absorb heavy metals (Alves *et al*, 2002; Ma *et al*, 2015), hence the greater discoloration (likely the result of oxides of Cu, Mn, Co, etc) is an indicator of bacterial activity. This colour change can be seen in Figure 30.

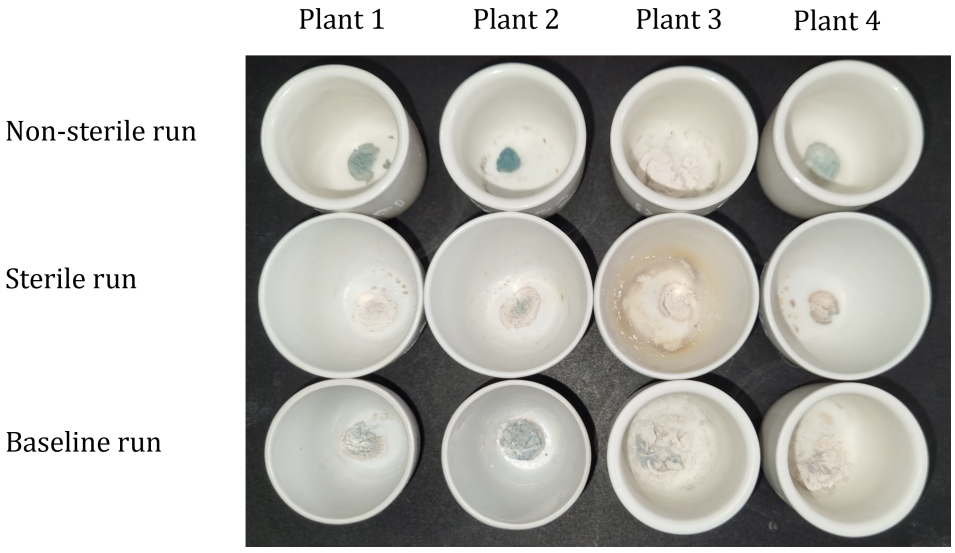


**Figure 30:** Photographs of the ash bearing crucibles after having been removed from the furnace.

Plant 3 of the non-sterile run also produced near pure white ash, implying that the plant lacked a bacterial colony. This is in line with the observed nitrogen uptake ratios where Plant 3 was seen to act far more like a plant from the sterile run than its peers in the non-sterile run, further supporting its exclusion from the "Non-sterile†" data set.

The second major difference between the two runs is the tendency of the dosing fraction and absorption fraction to diverge in the non-sterile run but not the sterile run. This can not simply be attributed to differing run-time as the absorbed and dosing fractions in

"Sterile*" line up almost perfectly. In fact, statistical analysis found that the difference in dosing fractions of nitrate were statistically significant between "Non-sterile†" and "Sterile*", yet absorption fractions were essentially the same. What this implies is that there is a consistent oversupply of ammonium (causing the accumulation seen in Figure 25) to the non-sterile run by the control system. This, in turn, suggests that the controller is trying to suppress some kind of upwards pH pressure, which means that something unexpected is absorbing protons. Other than normal microbial respiration (which should be at a minimum owing to the lack of a significant carbon source within the medium), the only other confounding factor at work here is the activity of nitrifying bacteria. This is an acidic reaction commonly believed to emit two protons for every ammonium molecule nitrified to nitrate (van Rooyen & Nicol, 2022b; Silber & Bar-Tal, 2008: 301), though some sources also suggest only one proton is released (van Rooyen, Brink, *et al*, 2021). If the actual proton ratio was less than 1.5, this would cause a basic response in the system at the high initial nitrate concentration of the system. This would prompt the controller to start adding ammonium in an attempt to push pH lower. The nitrification of some or all of the ammonium in conjunction with the general tendency of plants to absorb nitrate preferentially would cause the ammonium accumulation observed in Figure 25. The virtue of this explanation is evident by the prominent peak and subsequent decline visible in the pH of Pant 1 and Plant 2 in Figure 25 for the non-sterile run, where this turning point likely indicates an overshoot of the ammonium needed to bring pH back to the set point.

Regardless of these deviations, which in the grander scheme of things seem only to represent a slightly more bumpy pH profile and high ammonium fractions, the non-sterile run shows that the control system continues to deliver satisfactory pH control. Despite the high ammonium fractions, the system still delivered satisfactory yields of leaf material on par with the sterile and baseline runs, implying that ammonium toxicity was successfully avoided.

### 4.3.4 Nutritional analysis of the leaves

The results of the nitrate, ammonium, protein, and total nitrogen analyses are shown in Figure 31.

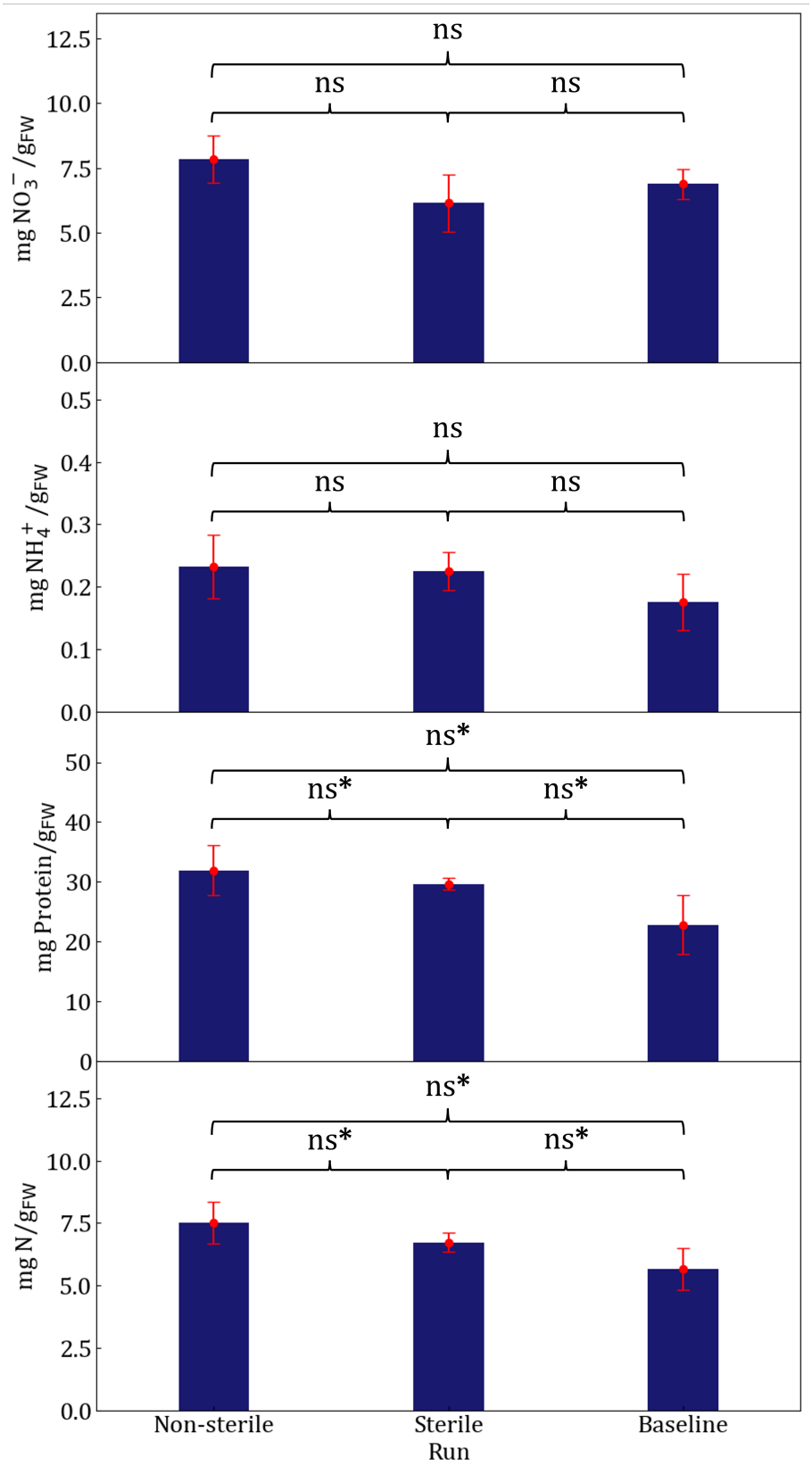


**Figure 31:** Content of nitrogenous species in the leaves on a fresh mass basis. ns means no significant difference according to t-testing. ns* refers to the case where ANOVA suggested a significant difference but t-testing did not.

While the results of the nitrate analysis are consistent with literature in that they show a decrease in the nitrate content from the baseline to the sterile run, it is important to note that the difference was not statistically significant. At the very least, this suggests that nitrate accumulation would not be any greater in the proposed system than for the conventional system. Similarly, while the non-sterile run showed a greater accumulation of nitrate, the difference as compared to the other runs was not statistically significant. While the values of nitrate content are certainly on the higher side of what can be found for similar species in literature (Song, L Li, *et al*, 2017), they do not strain credulity.

The ammonium analysis also hinted at possibly higher ammonium accumulation in the sterile and non-sterile runs when compared to the baseline run. While this makes sense considering they were fed ammonium, the results are not statistically significant and represent only a small fraction of the nitrogen present in the leaves.

The results of the protein analysis represent an interesting statistical dilemma. On one hand, ANOVA suggests that there is statistical significance between the sample populations. On the other, no individual population pairing was found to be sufficiently distinct from another within a 5 % confidence interval. This does not invalidate the results of the ANOVA, it simply means that we are unable to successfully identify between which groups the means differ significantly (Diez *et al*, 2019: 294). Looking at Figure 31, it is apparent that both the sterile and non-sterile runs accumulated more protein than the baseline run. Considering literature has found that plants fed on ammonium tend to generate more protein than those fed purely on nitrate (Song, L Li, *et al*, 2017; Zhang *et al*, 2007), this can be taken as tentative proof that the proposed system, through its simultaneous supply of ammonium and nitrate encourages protein synthesis.

The other nutritional aspect to consider is mineral content. The amount of mineral ions present in the leaves can be inferred from ashing analysis (*i.e.* by calculating the fraction of material left after ashing at high temperatures). The ash fractions are presented in Table 7.

**Table 7:** Results of the ash analysis

| | | Non-sterile | Sterile | Baseline |
|---|---|---|---|---|
| Wet basis | Average (%) | 1.59 | 1.53 | 1.66 |
| | StDev (%) | 0.105 | 0.124 | 0.074 |
| Dry basis | Average (%) | 16.6 | 16.9 | 18.5 |
| | StDev (%) | 1.1 | 1.5 | 0.9 |

The marginally higher ash content in the baseline run agrees with literature as it stands to reason that the increased competition from ammonium would suppress the movement

of other cations into the roots. However, ANOVA and t-testing revealed no statistical significance between the runs on a wet basis. As it stands, the ammonium/nitrate system is no better and no worse than the nitrate only system in this regard.

Finally, the chlorophyll content was analysed. The results are presented in Figure 32.

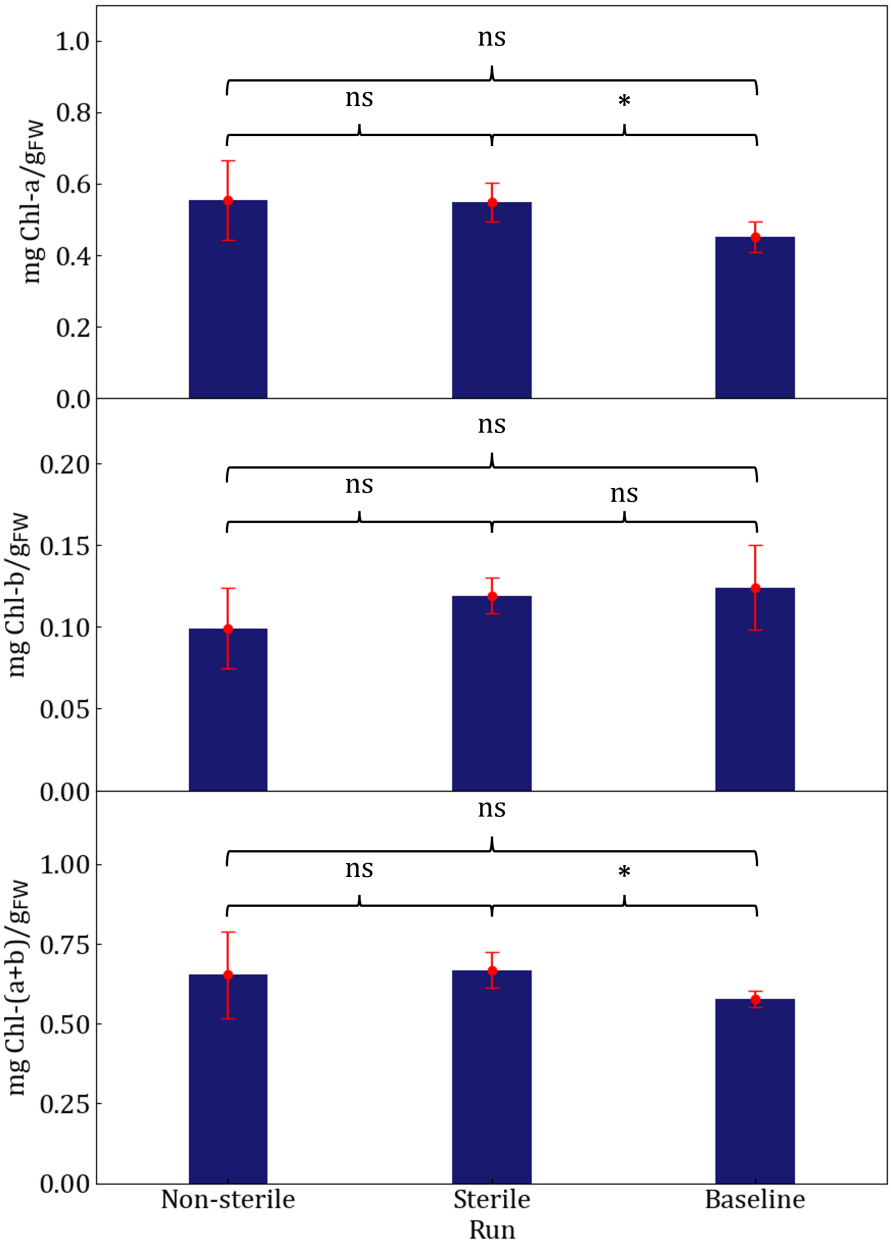


**Figure 32:** Chlorophyll content of leaves on a fresh mass basis. ns means no significant difference according to t-testing. * refers to cases where t-testing detected a statistically significant difference.

The chlorophyll contents appear reasonable when compared to literature (Yilmaz & Gökmen, 2016). While ANOVA failed to detect any significant difference, t-testing did. It is clear from Figure 31 that the sterile run showed a greater chlorophyll accumula-

tion than the baseline run. This is desirable, not only because greater concentrations of chlorophyll should make the plant more productive, but also because of the possible health benefits of chlorophyll (Juber, 2022). This increased accumulation of chlorophyll is corroborated with other studies which have found an increase in chlorophyll content with the addition of ammonium (Hu *et al*, 2015).

# 5 Conclusions and recommendations

As a means of controlling pH, the system is a success. pH was maintained close to the set point under both sterile and non-sterile conditions. EC was also maintained, though a more aggressive controller would probably be better, especially after the two week mark where the rate of nutrient absorption begins to outpace that of nutrient supply. Although the total nitrogen concentration was seen to decrease over time and the ammonium fraction in solution did on occasion breach the 50 % safety limit, there were no visible signs of ammonium toxicity. This is illustrated by the satisfactory growth rates achieved across all the runs. Moreover, despite the slightly depressed yield of leaves on a wet basis in the sterile and non-sterile runs, the dry leaf yield of both of these runs was very close to that of the baseline run, showing that the yield of edible plant matter is as good with the ammonium/nitrate system as with the conventional nitrate only system. While most literature on the subject of plant nutrition tends to find more convincing proof of statistically significant differences between ammonium/nitrate and nitrate only regimes, the sample size in this study was too small to attain statistical significance in many of the nutritional parameters measured. That being said, many of the findings mirrored that of literature and some statistically significant increases in protein and chlorophyll content were observed. Far from condemning this system, what the statistical analysis of the results revealed was that the nutritional parameters of the product plants were *at least* as good as those grown in pure nitrate, while avoiding any significant loss of yield.

The next logical step for a study into this type of control system would be to conduct experiments exceeding the three week period considered here so as to observe what effect the accumulation of the undesirable ions present in the baseline system would have. An alternative to this would be to reuse the nutrient solution in order to see if it will deleteriously affect new plants once their predecessors have been harvested. Moreover, the application of the proposed system in conjunction with organically sourced fertilisers would be an important step in creating a purely organic hydroponic system.

Possible improvements that can be made are further tuning of the pH control algorithm to try and reduce the tendency of the differential control to pin the pH and selecting more aggressive control parameters for the EC controller. It would also be informative to increase the operating time of the non-sterile run so as to see if the microbial interference would eventually be ironed out.

# References

Alves, ARA, Yin, Q, Oliveira, RS, Silva, EF and Novo, LAB (2002), "Plant growth-promoting bacteria in phytoremediation of metal-polluted soils: current knowledge and future directions", *Science of the Total Environment*, 838: 156435, DOI: https://doi.org/10.1016/j.scitotenv.2022.156435.

Arnon, DI (1949), "Copper enzymes in isolated chloroplasts. Polyphenoloxidase in *Beta vulgaris*", *Plant Physiology*, 24: 1–15.

Assimakopoulou, A, Salmas, I, Kounavis, N, Bastas, AI, Michopoulou, V and Michail, E (2019), "The impact of ammonium to nitrate ratio on the growth and nutritional status of kale", *Notulae Botanicae Horti Agrobotanici Cluj-Napoca*, 47 (3): 848–859.

Atmadja, W, Liawatimena, S, Lukas, J, Nata, EPL and Alexander, I (2017), "Hydroponic system design with real time OS based on ARM Cortex-M microcontroller", paper presented at*Proceedings of The International Conference on Eco Engineering Development 2017*, vol. 109, Earth and Environmental Science, IOP Publishing, Yogyakarta, Indonesia.

Barber, SA (1962), "A diffusion and mass-flow concept of soil nutrient availability", *Soil Science*, 93: 39–49.

Barberon, M and Geldner, H (2014), "Radial transport of nutrients: the plant root as a polarized epithelium", *Plant Physiology*, 166: 528–537.

Bentrup, F (2017), "Water ascent in trees and lianas: the cohesion-tension theory revisited in the wake of Otto Renner", *Protoplasma*, 254: 627–633.

Bloom, AJ (1988), "Ammonium and nitrate as nitrogen sources for plant growth", *ISI Atlas of Science: Animal and Plant Sciences*, 1 (1): 55–59.

Britto, DT and Kronzucker, HJ (2002), "$NH_4^+$ toxicity in higher plants: a critical review", *Journal of Plant Physiology*, 159: 567–584.

Bugbee, B (2004), "Nutrient management in recirculating hydroponic culture", *Acta Horticulturae*, 684: 99–112.

Chang, CL, Hong, GF and Fu, WL (2018), "Design and Implementation of a Knowledge-Based Nutrient Solution Irrigation System for Hydroponic Applications", *Transactions of the ASABE*, 61: 369–379.

Clark, DT (1974), *Ion Transport and Cell Structure in Plants*, McGraw-Hill, London, UK.

Cramer, MD and Lewis, OAM (1993), "The influence of $NO_3^-$ and $NH_4^+$ nutrition on the growth of wheat (Triticum aestivum) and maize (*Zea mays*) plants", *Annals of Botany*, 72: 359–365.

Cytryn, E, Levkovitch, I, Negreanu, Y, Dowd, S, Frenk, S and Silber, A (2012), "Impact of short-term acidification on nitrification and nitrifying bacterial community dynamics in soilless cultivation media", *Applied and Environmental Microbiology*, 78 (18): 6576–6582.

Dalton, FN (1984), "Dual pattern of potassium transport in plant cells: a physical artifact of a single uptake mechanism", *Journal of Experimental Botany*, 35 (161): 1723–1732.

Diez, D, C¸etinkaya-Rundel, M and Barr, CD (2019), *OpenIntro Statistics*, 4th ed., OpenIntro.

Dreyer, I and Michard, E (2020), "High- and low- affinity transport in plants from a thermodynamic point of view", *Frontiers in Plant Science*, 10 (1797).

Dunja Šamec, BU and Salopek-Sondi, B (2019), "Kale (Brassica oleracea var. acephala) as a superfood: Review of the scientific evidence behind the statement", *Critical Reviews in Food Science and Nutrition*, 59 (15): 2411–2422, DOI: 10.1080/10408398.2018.1454400.

Dunn, B and Singh, H (2016), *Electrical Conductivity and pH Guide for Hydroponics;* Technical report, Oklahoma State University: Stillwater, OK, USA.

element14 (2021), "Gaussian noise", URL: https://in.element14.com/gaussian-noise-definition (visited on 05/06/2021).

European Commoission (2023), *Commission regulation (EU) 2023/915 of 25 April 2023 on maximum levels for certain contaminants in food and repealing Regulation (EC) No 1881/2006*, Legal maximum limits of various contaminants in food products within the EU, Brussels.

Fallovo, C, Colla, G, Schreiner, M, Krumbein, A and Schwarz, D (2006), "Effect of nitrogen form and radiation on growth and mineral concentration of two *Brassica* species", *Scientia Horticulturae*, 123: 170–177.

Felle, HH (2001), "pH: signal and messenger in plant cells", *Plant Biology*, 3: 577–591.

Fernandes, D (2020), "A guide to different pH down options in hydroponics", URL: `https://scienceinhydroponics.com/2020/05/a-guide-to-different-ph-down-options-in-hydroponics.html` (visited on 10/29/2023).

Fernández, E and Cárdenas, J (1982), "Regulation of the nitrate-reducing system enzymes in wild-type and mutant strains of Chlamydomonas reinhardii", *Mol Gen Genet*, 186: 164–169.

Florencio, FJ and Vega, JM (1983), "Utilization of nitrate, nitrite and ammonium by Chlamydomonas reinhardii: Photoproduction of ammonium", *Planta*, 158 (4): 288–293.

Glass, ADM and Siddiqi, MY (1995), "Nitrogen Absorption by plant roots", In: Srivastava, H and Singh, R Ed., Nitrogen Nutrition in Higher Plants. 21–56.

Gorenjak, AH and Cencič, A (2013), "Nitrate in vegetables and their impact on human health: a review", *Acta Alimentaria*, 42 (2): 158–172.

Green, DW and Perry, RH (2008), *Perry's Chemical Engineers' Handbook*, 8th ed., McGraw-Hill, New York.

Hedrich, R and Schroeder, JI (1989), "The physiology of ion channels and electrogenic pumps in higher plants", *Plant Physiology*, 40: 539–569.

Hillel, D (2003), *Introduction to Environmental Soil Physics*, Academic Press/Elsevier, Cambridge, Massachusettes.

Hoagland, DR and Arnon, DI (1938), *The Water-Culture Metho for Growing Plants without Soil*, Circular 347 of the California Agricultural Experiment Station, College of Agriculture, University of California, Berkeley.

Hopmans, JW and Bristow, KL (2002), "Current capabilities and future needs of root water and nutrient uptake modelling", *Advances in Agronomy*, 77: 103–183.

Hu, L, Yu, J, Liao, W, Zhang, G, Xie, J, Lv, J, Xiao, X, Yang, B, Zhou, R and Bu, R (2015), "Moderate ammonium:nitrate alleviates low light intensity stress in mini Chinese cabbage seedling by regulating root architecture and photosynthesis", *Scientia Horticulturae*, 186: 143–153.

Ismande, J (1986), "Nitrate-ammonium ratio required for pH homeostasis in hydroponically grown soybean", *Journal of Experimental Botan*, 37 (176): 341–347.

Juber, M (2022), "Health benefits of chlorophyll", [2023-11-06], URL: `https://www.webmd.com/diet/health-benefits-chlorophyll`.

Kaewwiset, T and Yooyativong, T (2017), "Electrical conductivity and pH adjusting system for hydroponics by using linear regression", 14th International Conference on Electrical Engineering/Electronics, Computer, Telecommunications and Information Technology.

Kirkham, MD (2004), *Principles of Soil and Plant Water Relations*, Academic Press/Elsevier, Cambridge, Massachusettes.

Kotz, JC, Treichel, PM, Townsend, JR and Treichel, DA (2015), *Chemistry and Chemical Reactivity*, 9th ed., Cengage Learning, Stamford, Connecticut.

Kramer, PJ (1983), *Water Relations of Plants*, Academic Press, Cambridge, Massachusettes.

Kramer, PJ and Boyer, JS (1995), *Water Relations of Plants and Soils*, Academic Press, San Diego, California.

Labuschagne, A, van der Merwe, AJ, van Rensburg, NFJ and Zietsman, L (2018), *An Introduction to Numerical analysis*, 7th ed., Celtis Publisher, Pretoria, South Africa.

Lobit, P, López-Pérez, L, Cárdenas-Navarro, R, Castellanos-Morales, VC and Ruiz-Corro, R (2007), "Effect of ammonium/nitrate ratio on growth and development of avocado plants under hydroponic conditions", *Canadian Journal of Plant Sciences*, 87: 99–103.

Lu, N and Shimamura, S (2018), "Protocols, issues and potential improvements of current cultivation systems." chapter in *Smart Plant Factory: the Next Generation Indoor Vertical Farms*: 31–49.

Ma, Y, Rajkumar, M, Rocha, I, Oliveira, RS and Freitas, H (2015), "Serpentine bacteria influence metal translocation and bioconcentration of *Brassica juncea* and *Ricinus communis* grown in multi-metal polluted soils", *frontiers in Plant Science*, 5.

Maathuis, FJM (2009), "Physiological functions of mineral macronutrients", *Current Opinion in Plant Biology*, 12: 250–258.

Madigan, MT, Bender, KS, Buckley, DH, Sattley, WM and Stahl, DA (2022), *Brock Biology of Microorganisms: Global Edition*, 16th ed., Pearson, United Kingdom.

Masclaux-Daubresse, C, Daniel-Vedele, F, Dechorgnat, J, Chardon, F, Gaufichon, L and Suzuki, A (2010), "Nitrogen uptake, assimilation and remobilization in plants: challenges for sustainable and productive agriculture", *Annals of Botany*, 105: 1141–1157.

Mattaini, K (2020), *Introduction to Molecular and Cellular Biology*, Roger Williams University, Bristol, Rhode Island.

McFarlane, KJ and Yanai, RD (2006), "Measuring nitrogen and phosphorus uptake by intact roots of mature *Acer saccharum* Marsh., *Pinus resinosa* Ait., and *Picea abies* (L.) Karst", *Plant and Soil*, 279: 162–173.

Mengel, K, Kirkby, EA, Kosegrten, H and Appel, T (2001), *Principles of Plant Nutrition*, Kluwer Academic Publishers, Dordrecht, the Netherlands.

Mengel, K, Robin, P and Sal sac, L (1983), "Nitrate reductase in shoots and roots of maize seedlings as affected by the form of nitrogen nutrition and the pH of the nutrient solution", *Plant Physiology*, 71: 618–622.

Miller, A, Adhikari, R and Nemali, K (2020), "Recycling nutrient solution can reduce growth due to nutrient deficiencies in hydroponic production", *Frontiers in Plant Science*, 11.

Miller, AJ and Cramer, MD (2004), "Root nitrogen acquisition and assimilation", *Plant and Soil*, 274: 1–36.

Miller, S and Childers, D (2021), *Probability and Random Processes With Applications to Signal Processing and Communications*, 2nd ed., Elsevier, Amsterdam.

Mokobi, F (2022), "Plant cell- definition, structure, parts, functions, labeled diagram", URL: https://microbenotes.com/plant-cell/, [2022-11-08].

NIST (2023), "Two-sample t-test for equal means", [2023-11-06], URL: https://www.itl.nist.gov/div898/handbook/eda/section3/eda353.htm.

Patel, M (2022), "How to grow kale in hydroponics", URL: https://risehydroponics.in/how-to-grow-kale-in-hydroponics/, [2022-12-05].

Patterson, K, Cakmak, T, Cooper, A, Lager, I, Rasmusson, AG and Escobar, MA (2010), "Distinct signalling pathways and transcriptome response signatures differentiate ammonium and nitrate-supplied plants", *Plant, Cell and Environment*, 33: 1486–150.

Peters, WS, Jensen, KH, Stone, HA and Knoblauch, M (2021), "Plasmodesmata and the problems with size: Interpreting the confusion", *Journal of Plant Physiology*, 257: 153341.

Porra, RJ (2002), "The chequered history of the development and use of simultaneous equations for the accurate determination of chlorophylls a and b", *Photosynthesis Research*, 73: 149–156.

Ramazzotti, S, Gianquinto, G, Pardossi, A, Muñoz, P and Savvas, D (2013), *Good Agricultural Practices for Greenhouse Vegetable Crops: Principles for Mediterranean Climate Areas*, Guide on greenhouse vegetable production by the Food and Agricultural Organisation of the United Nations, Rome.

Raven, JA (1985), "Regulation of pH and generation of osmolarity in vascular plants: a cost-benefit analysis in relation to efficiency of use of energy, nitrogen and water", *New Phytologist*, 101: 25–77.

Ricca, C, Bhakay, BA, Shen, Y, Khusid, B and Dave, R (2012), *Water Potential ($\Psi$)*, Experimental guide on water potential for the New Jersey Institute of Technology, New Jersey.

Rubenstein, DA, Yin, W and Frame, MD (2021), *Biofluid Mechanics*, 3rd ed., Academic Press, Cambridge, Massachusettes.

Ruengittinun, S, Phongsamsuan, S and Sureeratanakorn, P (2017), "Applied internet of thing for smart hydroponic farming ecosystem (HFE)", *2017 10th International Conference on Ubi-media Computing and Workshops (Ubi-Media)*, 1–4.

Salsac, L, Chaillou, S, Morot-Gaudry, JF, Lesaint, C and Jolivoe, E (1987), "Nitrate and ammonium nutrition in plant", *Plant Physiology and Biochemistry*, 25: 805–812.

Santamaria, P (2006), "Nitrate in vegetables: toxicity, content, intakeand EC regulation", *Journal of the Science of Food and Agriculture*, 86: 10–17.

Saputra, RE, Irawan, B and Nugraha, YE (2017), "System design and implementation automation system of expert system on hydroponics nutrients control using forward chaining method", *2017 IEEE Asia Pacific Conference on Wireless and Mobile (APWiMob)*, 41–46.

Scherholz, ML and Curtis, WR (2013), "Achieving pH control in microalgal cultures through fed-batch addition of stoichiometrically-balanced growth media", *BMC Biotechnology*, 13 (39).

Seborg, DE, Edgar, TF, Mellichamp, DA and Doyle III, FJ (2017), *Process Dynamics and Control*, 4th ed., John Wiley & Sons, Inc., Hoboken.

Shaner, DL and S, BJ (1976), "Nitrate reductase activity in maize (*Zea mays* L.) leaves", *Plant Physiology*, 58: 499–504.

Silber, A and Bar-Tal, A (2008), "Nutrition of substrate grown plants", chapter in *Soilless Culture: Theory and Practice*: 291–339.

Song, S, Li, G, Sun, G, Liu, H and Chen, R (2016), "Uptake kinetics of different nitrogen forms by chinese kale", *Communications in Soil Science and Plant Analysis*, 47 (11): 1372–1378.

Song, S, Li, L, Zhu, Y, Liu, H, Sun, G and Chen, R (2017), "Effects of ammonium and nitrate ratios on plant growth, nitrate concentration and nutrient uptake in flowering chinese cabbage", *Bangladesh Journal of Botany*, 46 (4): 1259–1267.

Tabatabaei, S, Yusefi, M and Hajiloo, J (2008), "Effects of shading and NO3:NH4 ratio on the yield, quality and N metabolism in strawberry", *Scientia Horticulturae*, 116 (3): 264–272, DOI: https://doi.org/10.1016/j.scienta.2007.12.008.

The Editors of Encyclopaedia Britannica (2022), "Cell wall", URL: https://www.britannica.com/science/cell-wall-plant-anatomy/Proteins, [2022-11-08].

The Editors of Encyclopaedia Britannica (2023), "Osmotic pressure", URL: https://www.britannica.com/science/osmotic-pressure, [2023-11-24].

Torabizadeh, H (2011), "All proteins have a basic molecular formula", *International Journal of Chemical and Molecular Engineering*, 5 (6).

Tyree, MT (2003), "Plant hydraulics: the ascent of water", *Nature*, 423: 923–923.

Ullrich, WR (1992), "Transport of nitrate and ammonium through plant membranes", In: Mengel, K and Pilbeam, D J, Ed., Nitrogen Metabolism in Plants, Oxford University Press, Oxford: 121–137.

van Rooyen, IL, Brink, HG and Nicol, W (2021), "pH-based control strategies for the nitrification of high-ammonium wastewaters", *Fermentation*, 7 (4): 319.

van Rooyen, IL and Nicol, W (2021), "Optimal hydroponic growth of *Brassica oleracea* at low nitrogen concentrations using a novel pH-based control strategy", *Science of the Total Environment*, 775: 145875.

van Rooyen, IL and Nicol, W (2022a), "Inferential control of the phosphate concentration in hydroponic systems via measurement of the nutrient solution's pH-buffering capacity", *Scientia Horticulturae*, 295: 110820.

van Rooyen, IL and Nicol, W (2022b), "Nitrogen management in nitrification-hydroponic systems by utilizing their pH characteristics", *Environmental Technology and Innovation*, 26: 102360.

Velásquez-Yévenes, L and Ram, R (2022), "The aqueous chemistry of the copper-ammonia system and its implications for the sustainable recovery of copper", *Cleaner Engineering and Technology*, 9: 100515, ISSN: 2666-7908, DOI: https://doi.org/10.1016/j.clet.2022.100515.

Velazquez-Gonzalez, R, Garcia-Garcia, A, Ventura-Zapata, E, Barceinas-Sanchez, J and Sosa-Savedra, J (2022), "Review on hydroponics and the technologies associated for medium- and small-scale operations", *Agriculture*, 12 (5).

Wang, Y, Zhang, X, Liu, H, Sun, G, Song, S and Chen, R (2022), "High $NH_4^+/NO_3^-$ ratio inhibits the growth and nitrogen uptake of chinese kale at the late growth stage by ammonia toxicity", *Horticulturae*, 8 (1).

Wegner, LH and Shabala, S (2019), "Biochemical pH clamp: the forgotten resource in membrane bioenergetics", *New Phytologist*, 225 (1): 37–47.

Wenceslau, DdSL, de Oliveira, DF, Rabelo, HdO, Ferbonink, GF, Gomes, LAA, Leonel, ECA and Caione, G (2021), "Nitrate concentration and nitrate/ammonium ratio on lettuce grown in hydroponics in Southern Amazon", *African Journal of Agricultural Research*, 17 (6): 862–868.

Williams, KA and Nelson, JS (2016), "Challenges of using organic fertilizers in hydroponic production systems", *Acta Horticulturae*,

Xiaochuang, C, Lianghuan, W, Ling, Y, Xiaoyan, L, Yuanhong, Z and Qianyu, J (2015), "Uptake and uptake kinetics of nitrate, ammonium and glycine by pakchoi seedlings (*Brassica Campestris* L. *ssp. Chinensis* L. *Makino*)", *Scientia Horticulturae*, 186: 247–253.

Yilmaz, C and Gökmen, V (2016), "Chlorophyll", chapter in *Encyclopedia of Food and Health*: 31–47.

Zhang, F, Kang, S, Li, F and Zhang, J (2007), "Growth and major nutrient concentrations in *Brassica campestris* supplied with different $NH_4^+/NO_3^-$ ratios", *Journal of Integrative Plant Biology*, 49 (4): 455–462.

Zhao, L and Wang, Y (2017), "Nitrate assay for plant tissues", *Bio-protocol*, 7 (2).

Zhu, Y, Li, G, Liu, H, Sun, G, Chen, R and Song, S (2018), "Effects of partial replacement of nitrate with different nitrogen forms on the yield, quality and nitrate content of Chinese kale", *Communications in Soil and Plant Analysis*, 49 (11): 1384–1393.

# A Modelling equations

In order to reduce the amount of time spent tuning the controller, a dynamic model of the plant and its interaction with the system was designed. This consisted of a series of differential equations which were solved using the Euler method. The model specifically focused on ammonium, nitrate, and phosphate as the absorption and dissociation of these species account for the bulk of pH effects. In order to simulate the action of a discrete controller on a real system, the Euler method was applied with a time step of 1.38 s while

sampling and control action was applied every 30 min (this would correlate to about 1300 time steps between ever sampling point).

The differential equations applied to the physical model of the plant were

$$\frac{\mathrm{d}FW}{\mathrm{d}t} = -1.129 + 1.796t \tag{5}$$

$$\frac{\mathrm{d}N'_{\mathrm{NO_3^-}}}{\mathrm{d}t} = (FW)(RF)\frac{V_{max,\mathrm{NO_3^-}}C_{\mathrm{NO_3^-}}}{C_{\mathrm{NO_3^-}} + K_{m,\mathrm{NO_3^-}}} \tag{6}$$

$$\frac{\mathrm{d}N'_{\mathrm{NH_4^+}}}{\mathrm{d}t} = (FW)(RF)\frac{V_{max,\mathrm{NH_4^+}}C_{\mathrm{NH_4^+}}}{C_{\mathrm{NH_4^+}} + K_{m,\mathrm{NH_4^+}}} \tag{7}$$

$$\frac{\mathrm{d}N'_{\mathrm{P}}}{\mathrm{d}t} = \frac{1}{15}\left(\frac{\mathrm{d}N'_{\mathrm{NH_4^+}}}{\mathrm{d}t} + \frac{\mathrm{d}N'_{\mathrm{NO_3^-}}}{\mathrm{d}t}\right) \tag{8}$$

$$\frac{\mathrm{d}N'_{\mathrm{H^+}}}{\mathrm{d}t} = \frac{\mathrm{d}N'_{\mathrm{NH_4^+}}}{\mathrm{d}t} - 0.5\frac{\mathrm{d}N'_{\mathrm{NO_3^-}}}{\mathrm{d}t} \tag{9}$$

where $FW$ refers to fresh mass (g), $RF$ refers to the root fraction of the fresh mass (taken as 23 %), $t$ refers to time (days), $N'_i$ refers to the absorption of species $i$ by the plant (mmol). These differential terms were then multiplied by the time step to get the change of each component at each iteration. These changes were then integrated into mole balances that accounted for additions from the dosing reservoirs. These mole balances were

$$N_{\mathrm{NO_3^-},j} = N_{\mathrm{NO_3^-},j-1} - \frac{\mathrm{d}N'_{\mathrm{NO_3^-}}}{\mathrm{d}t}\Delta t + N_{\mathrm{NO_3^-},\mathrm{dosed}} \tag{10}$$

$$N_{\mathrm{NH_4^+},j} = N_{\mathrm{NH_4^+},j-1} - \frac{\mathrm{d}N'_{\mathrm{NH_4^+}}}{\mathrm{d}t}\Delta t + N_{\mathrm{NH_4^+},\mathrm{dosed}} \tag{11}$$

$$N_{\mathrm{P},j} = N_{\mathrm{P},j-1} - \frac{\mathrm{d}N'_{\mathrm{P}}}{\mathrm{d}t}\Delta t + N_{\mathrm{P},\mathrm{dosed}} \tag{12}$$

$N_{i,j}$ refers to the number of moles of species $i$ in solution at iteration $j$, $N_{i,\mathrm{dosed}}$ refers

to the number of moles of species $i$ dosed to the system. At every iteration other than sampling instances, $N_{i,\text{dosed}} = 0$.

EC was correlated to $[NH_4^+]$ and $[NO_3^-]$ using the expression

$$EC = 900 + 90[NO_3^-] + 70[NH_4^+] \tag{13}$$

where the 90 and 70 were estimated to be the contribution of the respective ions to EC and the 900 was the background EC contribution of a Hoagland solution mixture. These values were estimated by correlating data from various EC measurements of Hoagland solution in various depleted states.

The calculation of pH required a more involved treatment because the release/absorption of protons due to the action of ammonium/nitrate absorption would not only disturb the equilibrium between water and its dissociation products, but also the the equilibrium of phosphate. Even at the low phosphate concentrations involved in Hoaglands solution, phosphate buffering has a significant impact on pH, hence it had to be properly considered in the model. This was accomplished by modelling both the equilibrium of mono-basic and di-basic phosphate (the only two phosphate species that exist in the pH ranges considered) and the equilibrium of water.

The calculation of the equilibrium concentrations was performed using the procedure outlined by Kotz *et al* (2015: 642). The first step was to consider the individual phosphate species

$$N^*_{H_2PO_4^-,j} = N_{H_2PO_4^-,j-1} + N_{H_2PO_4^-,\text{dosed}} \tag{14}$$

$$N^*_{HPO_4^{2-},j} = N_{HPO_4^{2-},j-1} + N_{HPO_4^{2-},\text{dosed}} \tag{15}$$

where both of these values refer to the number of moles of phosphate in the system before equilibrium is re-established.

The reformation of $HPO_4^{2-}$ from $H_2PO_4^-$ is then assumed to go to completion where every proton generated by the absorption of nitrogen by the plant is assumed to be consumed. These values, along with the initial number of protons and hydroxide ions, are converted to concentrations and relabeled for the sake of brevity

$$\alpha = \frac{N^*_{\mathrm{HPO_4^{2-}},j} + N'_{\mathrm{H^+}}}{V}, \beta = \frac{N^*_{\mathrm{H_2PO_4^-},j} - N'_{\mathrm{H^+}}}{V}, \tau = 10^{\mathrm{pH_{j-1}}}, z = \frac{K_w}{10^{\mathrm{pH_{j-1}}}}$$

The phosphate is then considered to break up again, consuming $p$ moles of protons, as it achieves equilibrium. The water splitting reaction is then considered to go to equilibrium, producing $q$ moles of protons. The dissociation coefficient of phosphate ($K_P$, where $H_2PO_4^-$ forms $HPO_4^{2-}$) is known to be $6.2 \times 10^{-8}$ (Kotz *et al*, 2015: 637) and that of water ($K_w$) is $10^{-14}$ (Kotz *et al*, 2015: 539).

There are two unknowns ($p$ and $q$), and two equations (the equilibrium constants for $HPO_4^{2-}/H_2PO_4^-$ and $H_2O/H^+$, referred to as $K_P$ and $K_w$). The two equations are

$$K_P = \frac{[\mathrm{H^+}][\mathrm{HPO_4^{2-}}]}{[\mathrm{H_2PO_4^-}]} \tag{16}$$

$$= \frac{(p+q+\tau)(\alpha+p)}{(\beta-p)} \tag{17}$$

and

$$K_w = [\mathrm{H^+}][\mathrm{OH^-}] \tag{18}$$

$$= (p+q+\tau)(z+q) \tag{19}$$

Solving for $p$ and $q$ allows for the calculation of the equilibrium concentrations, taking into account the buffering capacity of phosphate and, at very low phosphate concentrations, the splitting of water. These values can then be used to calculate the pH for each iteration.

# B Statistical information

As was stated earlier, ANOVA and t-testing were performed on all the parameters assessed. For the sake of brevity data was said only to be significant or insignificant on a 5 % confidence interval in the main text. In this appendix, the actual p-values will be presented.

The p-values relating to the growth and yield data discussed in Section 4.3.2 are laid out in Table B.1.

**Table B.1:** p-values resultant from t-testing and ANOVA of the growth and yield parameters. Statistically significant results (p-values less than 5 %) are depicted in light green while those that are insignificant (p-values greater than 5 %) are depicted in light red.

| max RGR data | | |
|---|---|---|
| | t-test | ANOVA |
| Sterile vs non-sterile | 84.3% | |
| Sterile vs baseline | 84.9% | 97.1% |
| Non-sterile vs baseline | 95.4% | |
| **Leaf fraction (wet basis)** | | |
| | t-test | ANOVA |
| Sterile vs non-sterile | 80.3% | |
| Sterile vs baseline | 0.1% | 0.7% |
| Non-sterile vs baseline | 5.2% | |
| **Leaf fraction (dry basis)** | | |
| | t-test | ANOVA |
| Sterile vs non-sterile | 50.7% | |
| Sterile vs baseline | 7.3% | 9.6% |
| Non-sterile vs baseline | 8.2% | |
| **Total moisture fraction** | | |
| | t-test | ANOVA |
| Sterile vs non-sterile | 21.0% | |
| Sterile vs baseline | 3.5% | 16.1% |
| Non-sterile vs baseline | 91.6% | |

Similarly, the p-values relating to the nutritional data discussed in Section 4.3.4 are laid out in Table B.2.

**Table B.2:** p-values resultant from t-testing and ANOVA of the nutritional parameters. Statistically significant results (p-values less than 5 %) are depicted in green while those that are insignificant (p-values greater than 5 %) are depicted in red.

| Leaf nitrate content | | |
|---|---|---|
| | t-test | ANOVA |
| Sterile vs non-sterile | 6.2% | |
| Sterile vs baseline | 32.8% | 7.1% |
| Non-sterile vs baseline | 10.4% | |

| Leaf chlorophyll-a content | | |
|---|---|---|
| | t-test | ANOVA |
| Sterile vs non-sterile | 92.2% | |
| Sterile vs baseline | 3.4% | 15.3% |
| Non-sterile vs baseline | 16.1% | |

| Leaf ammonium content | | |
|---|---|---|
| | t-test | ANOVA |
| Sterile vs non-sterile | 84.9% | |
| Sterile vs baseline | 12.9% | 20.6% |
| Non-sterile vs baseline | 17.1% | |

| Leaf chlorophyll-b content | | |
|---|---|---|
| | t-test | ANOVA |
| Sterile vs non-sterile | 21.5% | |
| Sterile vs baseline | 70.2% | 26.6% |
| Non-sterile vs baseline | 20.2% | |

| Leaf N-protein content | | |
|---|---|---|
| | t-test | ANOVA |
| Sterile vs non-sterile | 58.0% | |
| Sterile vs baseline | 6.6% | 3.4% |
| Non-sterile vs baseline | 11.4% | |

| Leaf chlorophyll- a + b content | | |
|---|---|---|
| | t-test | ANOVA |
| Sterile vs non-sterile | 86.5% | |
| Sterile vs baseline | 3.8% | 31.6% |
| Non-sterile vs baseline | 33.6% | |

| Total N content | | |
|---|---|---|
| | t-test | ANOVA |
| Sterile vs non-sterile | 38.6% | |
| Sterile vs baseline | 7.5% | 3.0% |
| Non-sterile vs baseline | 11.5% | |

| Ash content (wet basis) | | |
|---|---|---|
| | t-test | ANOVA |
| Sterile vs non-sterile | 48.3% | |
| Sterile vs baseline | 14.0% | 26.9% |
| Non-sterile vs baseline | 34.5% | |

The statistics for the dosing and absorption ratios discussed in Section 4.3.3 are shown in Table B.3.

**Table B.3:** p-values resultant from t-testing and ANOVA of the absorption and dosing ratios of nitrate. Statistically significant results (p-values less than 5 %) are depicted in green while those that are insignificant (p-values greater than 5 %) are depicted in red.

| Nitrate dosing fraction | | |
|---|---|---|
| | t-test | ANOVA |
| Sterile vs non-sterile | 11.0% | 0.9% |
| Non-sterile vs non-sterile† | 41.5% | |
| Non-sterile vs sterile* | 16.8% | |
| Non-sterile† vs sterile* | 0.2% | |
| Sterile vs sterile* | 25.0% | |
| Sterile vs non-sterile† | 0.9% | |
| **Nitrate absorption fraction** | | |
| | t-test | ANOVA |
| Sterile vs non-sterile | 18.9% | 10.7% |
| Non-sterile vs non-sterile† | 51.1% | |
| Non-sterile vs sterile* | 80.5% | |
| Non-sterile† vs sterile* | 24.4% | |
| Sterile vs sterile* | 3.6% | |
| Sterile vs non-sterile† | 6.2% | |